DP-995

AEC RESEARCH AND DEVELOPMENT REPORT

IRRADIATION OF TUBULAR UO_2 FUEL ELEMENTS IN THE HWCTR

T. H. CRIM
G. R. COLE
W. G. HOLMES

REG. U. S. PAT. OFF.

Savannah River Laboratory

Aiken, South Carolina

Printed in the United States of America
Available from
Clearinghouse for Federal Scientific and Technical Information
National Bureau of Standards, U. S. Department of Commerce
Springfield, Virginia 22151
Price: Printed Copy $3.00; Microfiche $0.65

664401

DP-995

Reactor Technology
(TID-4500)

IRRADIATION OF TUBULAR UO_2 FUEL ELEMENTS IN THE HWCTR

by

T. H. Crim
G. R. Cole
W. G. Holmes

Work done by

G. R. Cole
T. H. Crim
W. W. West

Approved by

P. H. Permar, Research Manager
Nuclear Materials Division

November 1967

E. I. DU PONT DE NEMOURS & COMPANY
SAVANNAH RIVER LABORATORY
AIKEN, S. C. 29801

CONTRACT AT(07-2)-1 WITH THE
UNITED STATES ATOMIC ENERGY COMMISSION

ABSTRACT

Irradiation of 97 Zircaloy-clad urania tubes in the Heavy Water Components Test Reactor indicated that tubes with compacted powder cores made by the best available techniques will operate satisfactorily in a full-scale heavy-water-moderated power reactor to peak exposures of at least 20,000 MWD/MTU and peak thermal ratings ($\int_{T_s}^{T_c} kd\theta$) of 30 watts/cm. Examination of 45 tubes irradiated in the HWCTR indicated that:

1) Less than 10% of the fission gas produced during irradiation was released in fuel tubes operating at low $\int kd\theta$; the fractional release increased sharply with the onset of columnar grain growth in the urania core.

2) Release of nitrogen from impurities in fused urania was substantially reduced by outgassing the urania at high temperature in vacuum or hydrogen before irradiation.

3) The outer sheath wrinkled in tubes with relatively low-density cores [82-87% of theoretical density (TD)] operated at $\int kd\theta$ of 40-45 watts/cm; tubes compacted to 90% TD did not wrinkle when irradiated at 50 watts/cm.

CONTENTS

LIST OF TABLES AND FIGURES

List of Figures (Contd)

IRRADIATION OF TUBULAR UO_2 FUEL ELEMENTS IN THE HWCTR

INTRODUCTION

The development program on heavy-water-moderated power reactors sponsored by the U. S. Atomic Energy Commission had as its goal the advancement of the technology to the point that full-scale power plants could generate electricity at competitive costs. The Du Pont study was mainly directed toward heavy-water-moderated-and-cooled reactors. This program was terminated by the AEC at the end of FY-1965 in favor of a heavy-water-moderated, organic-cooled reactor.

Tubular fuel elements of urania received heavy emphasis in the Du Pont study because of the potentially low fabrication costs of such elements,[1] and their high melting point, resistance to attack by hot water, and relative dimensional stability under irradiation. Urania can be arc-fused and crushed to produce a powder of high particle density that can be compacted into an annulus between concentric tubes of Zircaloy to form fuel tubes of high bulk density. Compaction can be accomplished by vibration alone or by a combination of vibration and swaging. Tubes produced by both of these techniques were irradiated to permit correlation of in-reactor performance with fabrication variables and ultimately to determine the safe thermal rating and exposure limit of fuel elements.

This report summarizes the irradiation tests of compacted urania tubes in the Heavy Water Components Test Reactor (HWCTR) at Savannah River.

SUMMARY

Zircaloy-sheathed urania tubes fabricated by the best present techniques should operate satisfactorily in a full-scale heavy-water-moderated power reactor to peak exposures of at least 20,000 MWD/MTU* and peak thermal ratings** of 30 watts/cm. When the HWCTR irradiation program was terminated, two assemblies had attained peak exposures of 4,000 and 17,000 MWD/MTU at average peak*** ratings of 36 and 19 watts/cm, respectively. The most highly exposed elements in these assemblies were examined; results of the examination indicate that these elements would have operated satisfactorily to the goal exposures of 20,000 and 30,000 MWD/MTU, respectively.

Examination of more than 45 fuel tubes from nine irradiated assemblies and data from the irradiation of 10 other assemblies (not examined) indicated that:

1) In fuel tubes operating at low $\int k d\theta$, less than 10% of the fission gas produced during irradiation is released into the core voids.

2) The release of fission gas increases sharply at an $\int k d\theta$ of about 25-30 watts/cm, coincident with the onset of columnar grain growth in the urania core.

3) Columnar grain growth is extensive at 35 to 40 watts/cm, and central core melting occurs at about 60 watts/cm in swage-compacted tubes.

4) Release of gases from contaminants in fused urania, and consequent buildup of pressure in the fuel

* MWD/MTU = Megawatt days per metric ton of contained uranium (numerically equivalent to watt-days per gram of uranium).

** Thermal rating = $\int_{T_s}^{T_c} k d\theta$, an index of fuel temperature that is useful when precise values of the thermal conductivity are unknown.[2]

*** Average peak refers to the time-weighted average value at the axial location of the highest integrated exposure. Peak refers to the absolute maximum value in time and space.

element, can be substantially reduced by high-temperature vacuum outgassing or hydrogen treatment of the urania before irradiation.

5) The tubes will resist wrinkling of the outer sheath by the high coolant pressure, even at thermal ratings as high as 50 watts/cm if the urania core bulk density is 90% or higher. The outer sheaths of four tubes with relatively low-density cores (82-87%) wrinkled at thermal ratings of 40-45 watts/cm; such failures were avoided in later irradiations by compacting the tubes to densities of 90% and higher.

BACKGROUND

Initial irradiation tests of fuel tubes with compacted urania cores were performed in the Savannah River production reactors, which operated at cladding temperatures and coolant pressures substantially below those of interest for an economical full-scale power reactor. These tests included 7 assemblies that contained a total of 39 short tubes with outer and inner sheaths of Zircaloy. Seven of these tubes failed; detailed examinations of these tubes have been reported.[3,4] These examinations revealed two types of failure that were of particular significance in the development of a reliable fuel tube: 1) sheath cracking caused by embrittlement of the Zircaloy by hydrogen from the reaction of adsorbed moisture with impurities in the urania and 2) collapse of the inner sheath caused by excessive gas pressure in the voids in the core. Means of avoiding both these causes of tube failure were devised and incorporated in the procedures used for fabricating the tubes for subsequent irradiation tests.[5,6]

Prior to startup of the HWCTR, two Zircaloy-sheathed urania tubes were irradiated at power reactor conditions in the Vallecitos Boiling Water Reactor. Visual and dimensional examination of these tubes[7] indicated that their performance was satisfactory.

DESCRIPTION OF FUEL TUBES

The fuel tubes irradiated in the HWCTR contained an annular core of fused-and-crushed uranium dioxide compacted between outer and inner sheaths of Zircaloy-2. Carbon steel void chambers about 1 inch long were fabricated into the ends of each tube; these chambers contained perforated septums that separated the core from the void chamber and allowed passage of gases released from the core during irradiation. The ends of the tube were closed with Zircaloy-2 plugs welded to the sheaths by means of an inert-gas-shielded electric arc. The tubes, complete with welded end plugs, were evacuated through small vent holes and back-filled with helium; these holes were then sealed by welding.

The cores of some tubes were compacted by sonic vibration only to densities of 82 to 87 percent of theoretical; other tubes were further compacted by swaging over a mandrel to densities of 89 to 91 percent. The tubes were compacted in lengths of 4 to 10 feet; usually the compacted lengths were cut into ~14-inch sections to permit multiple irradiations in each reactor position, and to facilitate the postirradiation examination. Some 9-foot cores were also irradiated. Development of methods for fabricating these tubes has been described.[8-11]

The oxide tubes were fabricated to "base-case" sizes with outer diameters of approximately 2.1 inches or to "reference-design" sizes approximating the intermediate and large tubes of a 3-tube design of practical interest.[1] Average dimensions of the tubes in each of the irradiation tests are given in Table I; the comparative sizes of the base-case tubes and the reference-design tubes can be seen in Figure 1. The base-case tubes (SOT-1, SOT-2, SOT-5 and SOT-7 tests) were irradiated to explore the general behavior of powder-compacted UO_2 tubes and the effect of variations in fabrication practice and irradiation condition. Tubes of the reference design (SOT-6, SOT-8, SOT-9) were irradiated to demonstrate the behavior of tubes in the sizes of interest and to extend technology developed in earlier tests.

TABLE I

Average Dimensions of UO_2 Tubes Irradiated in the HWCTR

	Base Case								Reference Design	
	SOT-1[a]		OT-1[b]		SOT-2		SOT-5 SOT-7		Intermediate SOT-6 SOT-9	Large SOT-8
Dimension	V[c]	V+S[d]	V	V + S	V	V + S	V	V + S		
Outside Diameter, in.	2.060	2.062	2.060	2.062	2.153	2.121	2.152	2.121	2.540	3.651
Inside Diameter, in.	1.477	1.465	1.477	1.465	1.168	1.155	1.078	1.076	1.833	2.985
Sheath Thickness, in.										
Outer	0.029	0.029	0.029	0.029	0.030	0.034	0.030	0.033	0.023	0.036
Inner	0.031	0.031	0.031	0.031	0.038	0.037	0.038	0.037	0.023	0.032
Core Thickness, in.	0.232	0.238	0.232	0.238	0.424	0.411	0.470	0.455	0.308	0.260
Core Length, in.	11.38	11.38	111.4	111.4	10.84	10.84	10.75	10.75	10.75	9.88
Core Volume, $in.^3$	14.8	15.2	143.8	147.5	24.4	23.2	26.0	24.6	22.7	27.2
Void Volume (in end chambers), $in.^3$	1.08	1.08	1.08	1.08	3.40	3.30	3.67	3.54	2.65	2.74
Total Tube Length, in.	13.75	13.75	113.8	113.8	13.75	13.75	13.75	13.75	13.75	13.0

(a) SOT-1, etc. = Designations for the 14-inch segment of oxide tubes that comprise a single irradiation test in the HWCTR.
(b) OT-1 = Designation for the single tubes with 9-foot cores that comprise a single irradiation test in the HWCTR.
(c) V = Compacted by vibration.
(d) V + S = Compacted by vibration plus cold-swaging.

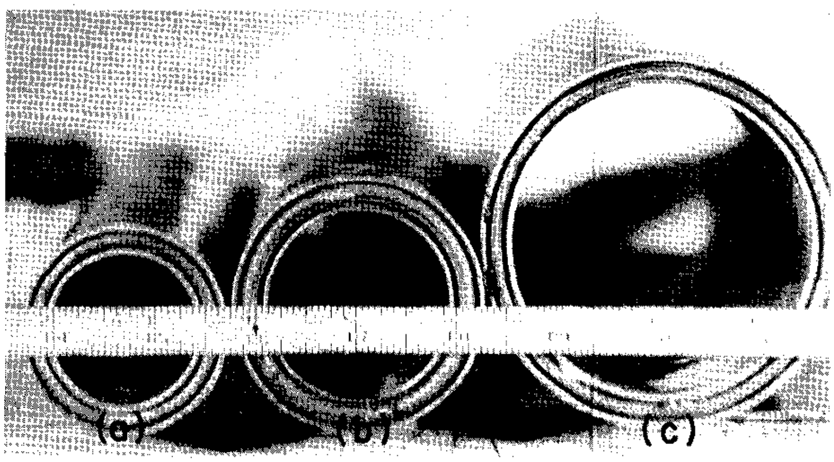

NEG. 66006

(a) Base case tube from SOT-1 test

(b) Intermediate size tube of reference design for SOT-6 test

(c) Large size tube of reference design from SOT-8 test

FIG. 1 TYPICAL UO_2 TUBES IRRADIATED IN THE HWCTR (½X)

The irradiation tests covered a range of operating conditions and element dimensions, and included several material variables (Tables I through VI). Wall thicknesses and uranium enrichments were chosen to provide successively higher thermal ratings ($\int kd\theta$), from the relatively low values of the SOT-1 test to values in the SOT-7 test that resulted in center melting. The uranium oxides used for these tubes were outgassed by heat treatments at various conditions to reduce the amounts of impurity gases.

IRRADIATION CONDITIONS

Information on the operating conditions of individual test assemblies and elements was obtained from calorimetric data from the HWCTR operating records that were processed by special computer codes to provide values for such parameters as $\int kd\theta$, specific power, heat flux, and exposure. The computer code provides a good approximation to the actual values of the various parameters at any axial location in the fuel column by computing individual values of the parameters for each of 19 equally spaced

TABLE II

Characteristics and Irradiation Conditions of UO_2 Tubes in SOT-1 Test

(Assemblies SOT-1-2 and SOT-1-3)

Tube No.[a]	Method of Compaction[b]	Core Density, % of Theoretical	∫kdθ, watts/cm Average in Time & Space	∫kdθ, watts/cm Peak	Exposure, MWD/MTU Average	Exposure, MWD/MTU Max.
SOT-1-2						
ZE-229E	V	85	6	18	5,000	6,600
ZE-225F	V + S	90	11	25	9,500	11,500
ZE-232E	V	84	16	25	13,500	15,400
ZE-222E	V + S	92	19	25	16,500	17,200
ZE-232D	V	84	18	24	16,700	17,200
ZE-225C	V + S	90	15	24	13,400	15,400
ZE-229F	V	85	8	18	7,400	10,400
SOT-1-3						
ZE-232F	V	84	6	14	2,900	3,700
ZE-225A	V + S	90	12	20	5,200	6,300
ZE-228D	V	84	17	23	7,600	8,600
ZE-225E	V + S	90	21	25	9,100	9,400
ZE-228G	V	86	20	25	9,100	9,400
ZE-222G	V + S	91	17	22	7,300	8,300
ZE-228B	V	84	9	17	4,100	5,600

(a) All tubes contained stoichiometric UO_2 enriched to 1.5% ^{235}U. All oxide was vacuum outgassed for 1 hour at 900-1000°C. Sheath material was low-nickel Zircaloy-2.

(b) V = Compacted by vibration only; V + S = Compacted by vibration plus swaging.

TABLE III

Characteristics and Irradiation Conditions of UO_2 Tubes in SOT-2 Test

(Assemblies SOT-2-2 and SOT-2-3)

Tube No.[a]	Method of Compaction	Core Density, % of Theoretical	∫kdθ, watts/cm Average in Time & Space	∫kdθ, watts/cm Peak	Exposure, MWD/MTU Average	Exposure, MWD/MTU Max.
SOT-2-2						
Z-257C[b]	V + S	89	3	10	300	500
Z-250B	V	83	12	26	900	1300
Z-256A	V + S	90	24	43	1900	2400
Z-251A[c]	V	87	37	49	2900	3300
Z-251C[c,d]	V	82	44	50	3400	3500
Z-255B	V + S	90	40	48	3200	3400
Z-257B[b]	V + S	89	30	41	2400	2900
Z-252C	V	82	16	25	1100	1600
SOT-2-3						
Z-254A	V + S	90	3	7	200	400
Z-251B	V	83	10	20	800	1000
Z-256B	V + S	90	21	34	1500	2000
Z-252B[c]	V	83	35	47	2400	2800
Z-254B	V + S	90	41	48	3100	3200
Z-253C[c,d]	V	85	41	48	3000	3100
Z-257A[b]	V + S	89	31	40	2300	2500
Z-253B	V	85	16	29	1200	1600

(a) All tubes contained stoichiometric UO_2 of natural enrichment that was vacuum outgassed for 4 hours at 1500-1600°C.

(b) Sheath material was Zircaloy-2; all other tubes fabricated with low-nickel Zircaloy-2 sheaths.

(c) Longitudinal wrinkle formed in outer sheath during irradiation.

(d) Outer sheath cracked at apex of wrinkle.

TABLE IV

Characteristics and Irradiation Conditions of UO_2 Tubes in SOT-5 and SOT-7 Tests

(Assemblies SOT-5-2 and SOT-7-2)

Tube No.	Oxide Treatment or Type(a)	Method of Compaction	Core Density, % of Theoretical	∫kdθ, watts/cm Average in Time & Space	∫kdθ, watts/cm Peak	Exposure, MWD/MTU Average	Exposure, MWD/MTU Max.
SOT-5-2							
Z-262A(b)	VO	V	86	14	35	400	600
Z-260C	HT(1750)	V + S	90	25	52	900	1000
Z-259C	VO	V + S	89	39	55	1300	1500
Z-259D(d)	VO	V + S	90	49	56	1600	1700
Z-261D	Hypostoichiometric	V + S	89	49	56	1600	1700
Z-261B	Hypostoichiometric	V + S	89	39	50	1300	1500
Z-262B(b)	VO	V	85	23	34	700	1000
SOT-7-2							
Z-265C	VO	V + S	90	8	12	100	200
Z-261C	Hypostoichiometric	V + S	90	14	23	200	300
Z-260B	HT(1750)	V + S	89	24	41	400	500
ZE-266C(c)	VO	V + S	89	50	66	800	1000
ZE-266A(c,e)	VO	V + S	91	64	68	1100	1100
Z-264A(f)	HT(1300)	V + S	90	49	54	800	900
Z-265B	VO	V + S	90	31	45	600	700

(a) VO - Stoichiometric UO_2 vacuum outgassed 4 hours at 1500-1600°C.
HT() - Stoichiometric UO_2 annealed in hydrogen for 12 hours at 1750°C or 4 hours at 1300°C as indicated.
Hypostoichiometric - Untreated arc-fused UO_2 with average O/U of 1.98.

(b) Sheath material was low-nickel Zircaloy-2; all other tubes fabricated with Zircaloy-2 sheaths.

(c) Enriched to 0.9% ^{235}U by blending natural UO_2 with 1.5% enriched UO_2; all other tubes fabricated with UO_2 of natural enrichment.

(d) Failed during irradiation when crack occurred in outer sheath through local area of severe hydriding located on outer surface of sheath; cause of hydriding unknown.

(e) Failed during irradiation when hole formed in inner sheath at top of tube over steel end chamber. Molten UO_2 had penetrated into the void chamber in this region during irradiation and may have caused excessive temperatures that resulted in sheath failure.

(f) The computed values of ∫kdθ for this tube are believed to be low because postirradiation examination shows that center melting occurred in this tube. Center melting also occurred in the two tubes in this assembly that contained enriched UO_2; in these tubes, center melting began at ∫kdθ of about 60 watts/cm. The error in the computed ∫kdθ values is attributed to assumptions made to simplify the calculation of power generation in UO_2 tubes containing different enrichments in the same assembly.

TABLE V

Characteristics and Irradiation Conditions of UO_2 Tubes of Intermediate Reference Size

(Assemblies SOT-6-2 and SOT-9-2)

Tube No.[a]	Core Density, % of Theoretical	∫kdθ, watts/cm Average in Time & Space	∫kdθ, watts/cm Peak	Exposure, MWD/MTU Average	Exposure, MWD/MTU Max.
SOT-6-2[b]					
Z-275A	90	6	19	1300	1700
Z-279B	92	11	27	2600	3000
Z-273A	91	18	28	3800	4300
Z-278C	91	22	28	4900	5100
Z-272C	91	22	27	4800	5000
Z-273C	91	18	24	3800	4400
Z-275C	91	9	15	2000	2800
SOT-9-2[b]					
ZE-283A	92	13	24	1500	1900
ZE-282A	92	24	34	2600	3100
ZE-281B	92	32	38	3500	3900
ZE-280C	91	36	40	4000	4000
ZE-299A	92	33	40	3700	4000
ZE-283B	92	25	34	2800	3200
ZE-283C	91	14	22	1400	2100

(a) All tubes contain stoichiometric UO_2 vacuum outgassed for 4 hours at 1300-1400°C, have Zircaloy-2 sheaths, and were compacted by vibration plus swaging.
(b) SOT-6 tubes contain UO_2 of natural enrichment. SOT-9 tubes are identical in size, but are enriched to 1.2% ^{235}U by mechanically blending natural UO_2 with 1.5% enriched UO_2.

TABLE VI

Characteristics and Irradiation Conditions of UO_2 Tubes of Large Reference Size

(Assembly SOT-8-3)

Tube No.[a]	Core Density, % of Theoretical	∫kdθ, watts/cm Average in Time & Space	∫kdθ, watts/cm Peak	Exposure, MWD/MTU Average	Exposure, MWD/MTU Max.
SOT-8-3					
ZE-297A	89	10	21	1400	1800
ZE-289A	92	18	29	2600	3200
ZE-297C	91	25	30	3800	4100
ZE-297B	92	29	33	4300	4300
ZE-290B	91	26	32	3900	4200
ZE-289D	92	19	28	3000	3400
ZE-290A	90	10	16	1600	2200

(a) All tubes -

- contain stoichiometric UO_2 that was enriched to 1.2% ^{235}U by mechanically blending natural UO_2 with 1.5% enriched UO_2 and was vacuum outgassed for 4 hours at 1300-1400°C.
- were fabricated with Zircaloy-2 sheaths.
- were compacted by vibration plus swaging.

locations between the top and bottom of the fuel column. Plots of three important parameters, the $\int kd\theta_{max}$, the time-weighted average $\int kd\theta$ (very nearly equal to exposure-weighted values), and the total exposure, are shown for each assembly in Appendix A. Experimental procedures are described in Appendix B.

For three of the assemblies SOT-1-2, SOT-2-2, and SOT-2-3 (Figures A-1, A-4, and A-5), isotopic analyses of core samples from the irradiated fuel tubes provided confirmation of the cumulative exposures as obtained by calculation from the calorimetric data. It is seen that agreements between the two sets of data are good. Most of the analytical values are slightly higher than the calculated values; the average difference is only 4%, although the differences are as large as 15% at the ends of the columns, where the exposures are small.

RESULTS

EFFECT OF CORE DENSITY AND THERMAL RATING ON OUTER SHEATH WRINKLING

The outer sheaths of four tubes with core densities of 82 to 87% formed longitudinal wrinkles during irradiation[12] (Figure 2). On two of these tubes (one each in the SOT-2-2 and SOT-2-3 assemblies), deformation of the sheath at the apex of the ridge was severe enough to cause small cracks (Figure 3) which released fission gases to the reactor coolant and required discharge of the assemblies. The core density and thermal rating of the tubes with wrinkled outer sheaths are plotted in Figure 4, together with the data for 32 other tubes that operated without deformation of their outer sheaths. The correlations shown in Figure 4 indicate that tubes compacted to core densities of 80 to 85% of theoretical can be operated safely at thermal ratings of about 25 watts/cm, and that an increase in the density to about 90% of theoretical or greater is required for satisfactory operation at thermal ratings of 40 to 50 watts/cm. The data were not sufficient to evaluate the effect of exposure or tube size; however, higher exposures and actual dimensions of interest in power reactor service are not expected to affect the conclusions from the present tests on UO_2 tubes irradiated to about 3,000 MWD/MTU.

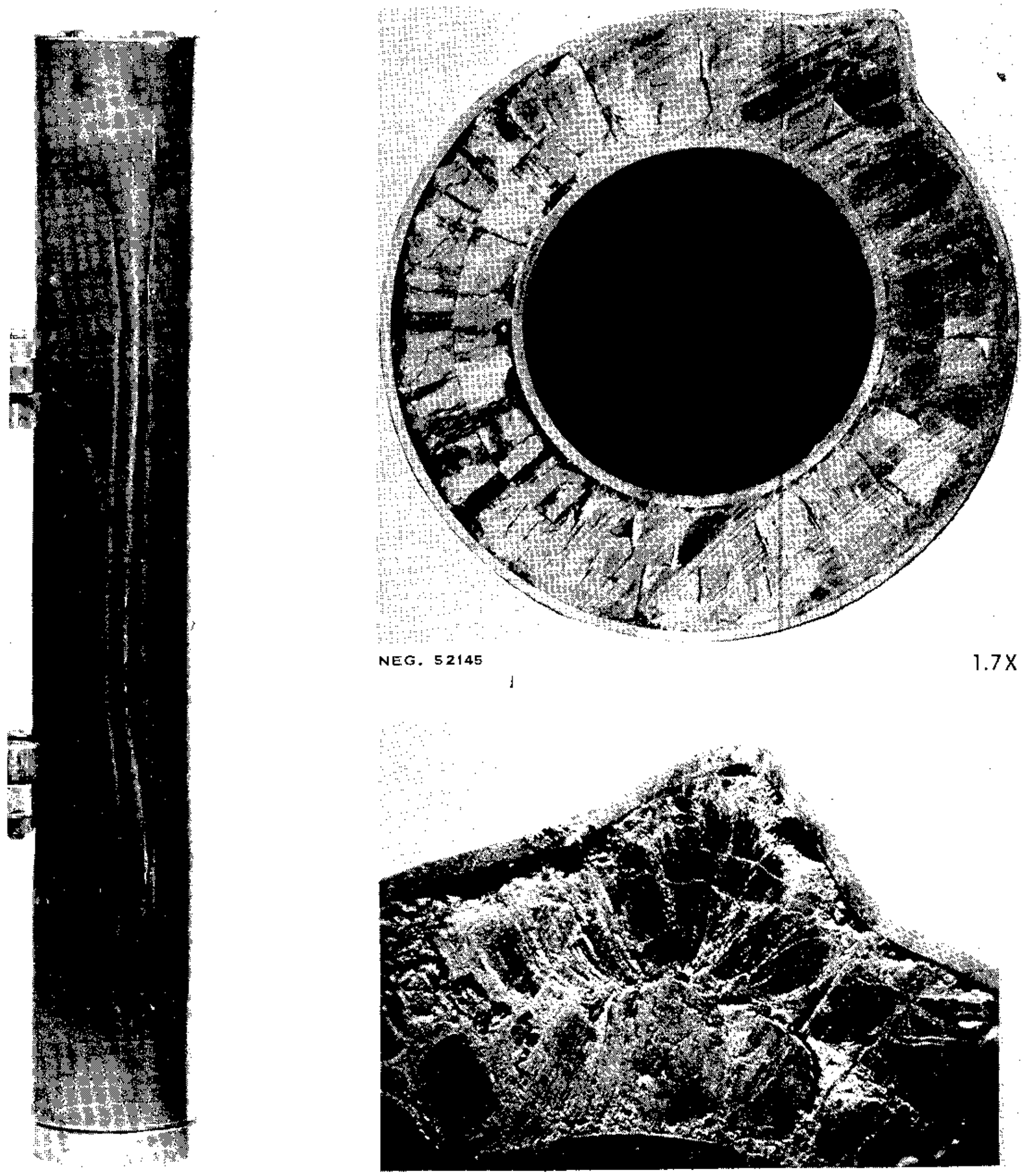

NEG. 52108 0.4X

a. Surface Appearance

NEG. 52145 1.7X

NEG. 52042 3.8X

b. Core Section

FIG. 2 TUBE FAILURE BY WRINKLING OF OUTER SHEATH

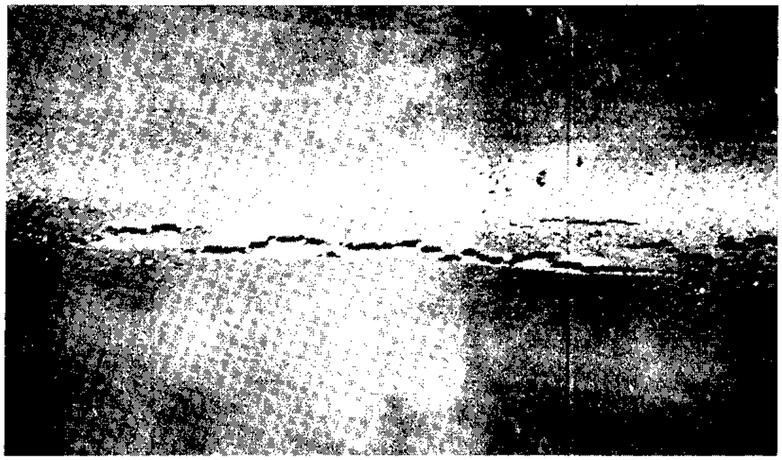

FIG. 3 SHEATH CRACKS AT APEX OF WRINKLE IN OUTER SHEATH

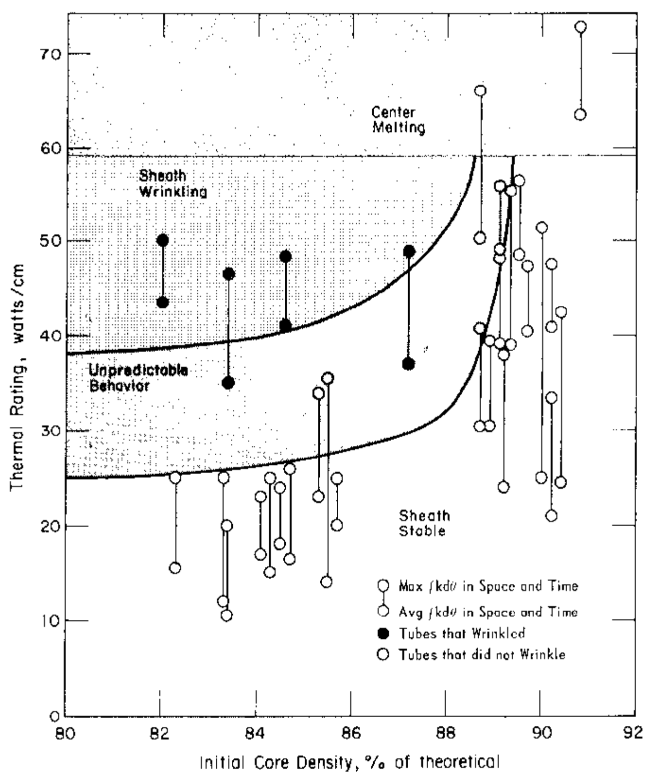

FIG. 4 EFFECT OF THERMAL RATING AND CORE DENSITY ON OUTER SHEATH WRINKLING OF UO_2 TUBES. (Four tubes that experienced outer sheath wrinkling and formed lengthwise ridges (Fig. 2) lie in a "Wrinkling Region" on the graph. Core melting occurred in two other tubes. (Diameter/thickness of the outer sheath is 70 for all tubes shown in the figure.)

The reduction in core volume accompanying the sheath wrinkling depended inversely on the initial bulk density of the urania; the core volume decrease ranged from 9% for the 82% dense tube to 2% for the 87% dense tube (see Table XIV, page 28). The stabilization of these cores at final densities of about 90% is consistent with the finding (Figure 4) that cores with densities above 90% are stable with respect to outer sheath wrinkling at the highest thermal ratings tested.

The core structure of wrinkled tubes indicates that the UO_2 became sufficiently plastic to allow the wrinkles to form by creep collapse induced by the coolant pressure (1200 psi). Both the distribution of UO_2 that had not undergone grain growth, and deformation of the columnar grains at the wrinkle indicate that sheath and core deformed as a unit with little relative movement at the core-sheath interface (Figure 5). The wrinkle is believed to have

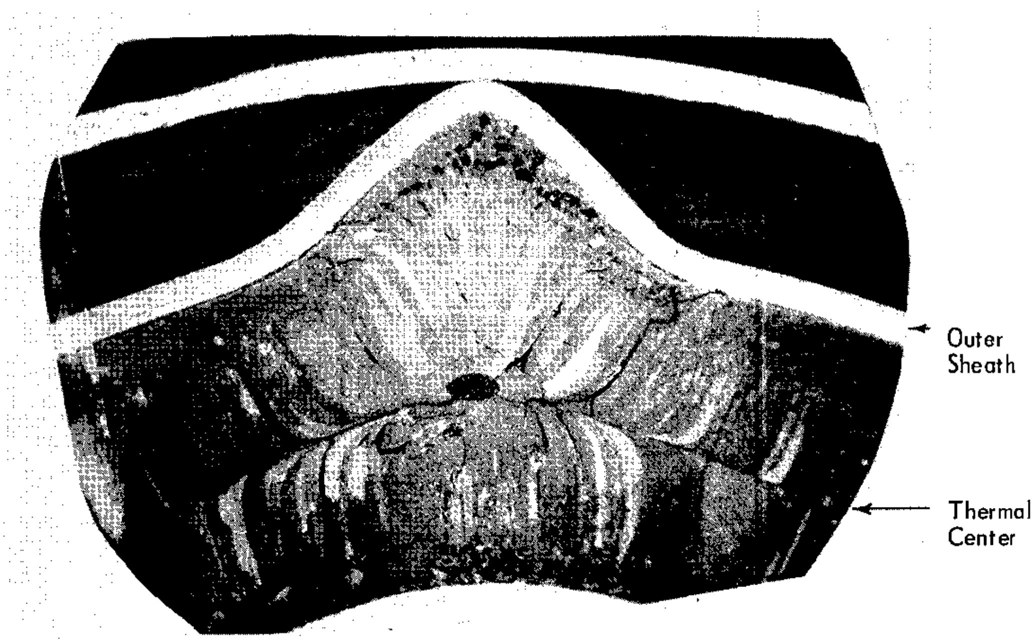

Note grain deformation along thermal center indicating lateral movement of UO_2 into the region of the wrinkle and then vertical movement toward the wrinkle. Tube Z-252B.

FIG. 5 CORE STRUCTURE AT WRINKLE IN OUTER SHEATH OF UO_2 TUBE initiated early in the irradiation and to have proceeded at a decreasing rate determined by the creep strength of the UO_2 core; as wrinkling proceeded, the core was also densifying and plasticity was decreasing. Sheath failures occurred at the apex of the wrinkle in two severely wrinkled tubes; these failures occurred during shutdown or startup after a shutdown, when sheath temperatures were low and stresses were high.

EFFECT OF OXIDE TREATMENT AND THERMAL RATING ON GAS RELEASE

The principal components of the gas mixture found in the void spaces of the fuel tubes after irradiation were xenon, nitrogen, and helium. Xenon and smaller quantities of krypton are fission products; nitrogen is generally an impurity in fused UO_2.[13] Helium was admitted to the evacuated fuel tube prior to final sealing; traces of argon from TIG welding were also admitted during fabrication. The gas contents of irradiated tubes are summarized in Tables VII through XI.

The xenon released, as a percentage of that formed in irradiation, depended primarily on the operating thermal rating, as shown in Figure 6. The sharp increase in xenon release above 25 watts/cm was associated with columnar grain growth in the urania cores. The effects of core density or exposure on the observed fractional release of xenon were minor.

Nitrogen gas released from the fused urania during irradiation ranged from 0.03 to 101 cc (STP) per kg of UO_2. The influence of preirradiation treatment of the urania on nitrogen release in-pile is shown in Table XII. High-temperature treatments of fused urania in either vacuum or hydrogen were effective in reducing both the nitride content and the amount of nitrogen released during irradiation. Hypostoichiometric UO_2, with no preirradiation treatment, released extremely small amounts of nitrogen during irradiation. The table includes elements irradiated under a wide range of conditions, but these variations appeared less important than the effect of pretreatment.

TABLE VII

Free Gas in Irradiated UO_2 Tubes from SOT-1 Tests
(Assemblies SOT-1-2 and SOT-1-3)

Tube No.	Gas Release (Major Constituents Only), cc/kg UO_2 Total	Xe	Kr	N_2	O_2	He	Ar	CO_2	Volume of He + Ar, cc at STP	Initial Free Volume, cc	Xenon Release, % of That Produced by Fission
Assembly SOT-1-2											
ZE-229E[a]											
ZE-225F[a]											
ZE-232E[a]											
ZE-222E	68	19.1	3.2	21	0.26	19.1	3.2	0.05	54	39	4.8
ZE-232D	224	84.0	13.3	97	0.18	21.7	7.1	0.24	64	55	21
ZE-225C	73	25.3	2.1	29	0.05	15.7	0.5	0.05	39	40	7.8
ZE-229F	23	3.7	0.3	0.2	0.03	18.4	0.3	0.01	41	54	2.1
Assembly SOT-1-3											
ZE-232F	48	0.90	0.14	26	0.17	20.1	1.0	0.05	47	55	1.3
ZE-225A	97	3.14	0.52	74	0.10	15.7	3.0	0.04	43	41	2.5
ZE-228D	94	5.70	0.90	61	0.33	24.7	1.4	0.04	58	56	3.1
ZE-225E	135	13.8	2.1	101	0.08	13.6	4.5	0.05	44	41	6.4
ZE-228G	136	22.2	3.8	83	0.43	26.1	0.2	0.05	59	53	10
ZE-222G	76	7.10	1.1	49	0.05	15.4	3.5	0.03	45	40	4.0
ZE-228B	93	1.82	0.31	66	0.21	23.8	0.50	0.02	54	56	1.8

(a) Not examined.

TABLE VIII

Free Gas in Irradiated UO_2 Tubes from SOT-2 Test
(Assemblies SOT-2-2 and SOT-2-3)

Tube No.	Gas Release (Major Constituents Only), cc/kg UO_2 at STP: Total	Xe	N_2	D_2[a]	He	Ar	Volume of He + Ar, cc at STP	Initial Free Volume, cc	Xenon Release, % of That Produced by Fission
Assembly SOT-2-2									
257C	23.5	0.05	0.7	ND	23	0.1	86	96	0.6
250B	31.0	1.1	0.3	ND	29	0.6	107	122	0.5
256A	48.8	4.8	16	ND	26	0.1	97	90	10
251A	69.2	31	5.6	ND	28	1.3	111	107	45
251C	Gas lost via sheath cracks								-
255B	69.2	39	0.2	ND	26	0.1	94	92	50
257B	40.2	14	5.0	ND	16	0.2	56	96	24
252C	31.5	ND	1.0	ND	30	0.03	109	126	-
Assembly SOT-2-3									
254A	30.4	0.06	6.0	ND	24	0.3	86	92	1.1
251B	30.3	0.3	1.5	ND	27	1.3	104	122	1.6
256B	29.6	0.9	4.5	ND	24	0.1	88	91	2.5
252B	76.4	29	11	ND	32	0.2	117	118	48
254B	302	27	23	218[b]	30	0.2	112	91	35
253C	Gas lost via sheath cracks								-
257A	50.0	13	5.7	ND	28	0.3	102	96	23
253B	26.6	0.3	5.9	ND	16	2.5	71	117	1.0

(a) "ND" signifies none detected.
(b) Presence of deuterium indicates that coolant leaked into the element during irradiation. Pressurization of the element with helium during the postirradiation examination failed to locate the leak site.

TABLE IX

Free Gas in Irradiated UO_2 Tubes in SOT-5 and SOT-7 Tests

(Assemblies SOT-5-2 and SOT-7-2)

Tube No.	Gas Release (Major Constituents Only), cc/kg UO_2 Total	Xe	N_2	He	Ar	Volume of He + Ar, cc at STP	Initial Free Volume, cc	Xenon Release, % of That Produced by Fission
Assembly SOT-5-2								
Z-262A	27.3	0.19	3.0	22.6	1.25	96	122	1.7
Z-260C	24.9	2.06	0.16	21.8	0.49	89	99	10
Z-259C	39.1	10.6	0.35	22.8	3.68	78	101	34
Z-259D	Gas lost through hole in sheath					-	101	-
Z-261D	36.9	10.6	0.05	22.5	2.07	96	101	27
Z-261B	27.1	3.69	0.03	22.0	0.97	88	102	12
Z-262B	28.2	0.37	3.5	23.0	1.18	97	123	2.1
Assembly SOT-7-2								
Z-265C	(a)	-	-	-	-		97	-
Z-261C	20.9	0.05	0.05	20.4	0.39	82	100	0.9
Z-260B	21.7	0.47	0.13	20.5	0.45	83	102	4.7
ZE-266C	(b)	-	-	-	-	-	102	-
ZE-266A	(c)	-	-	-	-	-	96	-
Z-264A	24.1	6.45	1.23	13.8	1.59	62	99	32
Z-2[illegible]5B	32.1	1.20	12.6	17.0	1.07	72	97	8.4

(a) Over half the collected sample consisted of H_2, HD, and D_2; of the remainder, 10% was fission gas and 25% was helium and argon. Anomalous behavior of the pressure of the gas sample prevented a determination of the amount of gas collected. The pressure rose unusually slowly during collection and continued to rise in the sample bulb when the bulb was removed from the sampling system. This behavior is believed to result from D_2O and H_2O vapor collected with the sample.

(b) The gas sample contained about 61% nitrogen, 22% oxygen, 16% helium and argon, 0.2% carbon dioxide, and 0.1% fission gas. The sample was collected normally, but is believed to have picked up air between the time of gas collection and analysis (the sample pressure increased from 47 to 75 mm Hg). A reliable correction for inleakage of air is not possible, however, for the nitrogen and oxygen contents were much larger than could be accounted for by the observed pressure rise.

(c) Failed during irradiation; no gas sample available.

TABLE X

Free Gas in Irradiated UO_2 Tubes of Intermediate Reference Size

(Assemblies SOT-6-2 and SOT-9-2)

Tube No.	Gas Release (Major Constituents Only), cc/kg UO_2 Total	Xe	Kr	N_2	O_2	He	Ar	CO_2	Volume of He + Ar, cc at STP	Initial Free Volume, cc	Xenon Release, % of That Produced by Fission
Assembly SOT-6-2											
Z-275A[a]											
Z-279B[a]											
Z-273A	37	4.2	0.4	12	0.06	19.3	1.0	0.0	76	76	4.0
Z-278C	48	11.6	0.9	14	0.05	21.1	0.8	0.02	79	77	9.5
Z-272C	35	11.6	0.9	5	0.04	16.4	1.0	0.1	64	77	9.5
Z-273C	40	5.0	0.4	14	0.1	19.4	1.4	0.02	72	76	4.8
Z-275C[a]											
Assembly SOT-9-2											
ZE-283A[a]											
ZE-282A	51	7.6	0.7	20	0.12	21.3	0.6	0.01	79	73	12
ZE-281B	68	19.7	3.2	22	0.07	21.3	0.5	0.05	82	74	24
ZE-280C	90	40.0	3.4	25	0.45	20.6	0.1	0.06	76	76	42
ZE-299A[a]											
ZE-283B[a]											
ZE-283C[a]											

(a) Not examined.

TABLE XI

Free Gas in Irradiated UO_2 Tubes of Large Reference Size
(Assembly SOT-8-3)

Tube No.	Gas Release (Major Constituents Only), cc/kg UO_2: Total	Xe	Kr	N_2	O_2	He	Ar	CO_2	Volume of He + Ar, cc at STP	Initial Free Volume, cc	Xenon Release, % of That Produced by Fission
Assembly SOT-8-3											
ZE-297A[a]											
ZE-289A[a]											
ZE-297C[a]											
ZE-297B	40	12.0	1.0	8	0.04	17.4	1.1	0.02	83	83	11.6
ZE-290B	40	9.6	0.8	13	0.02	15.8	0.4	0.02	72	84	10.2
ZE-289D	34	3.4	0.3	14	0.22	15.7	0.9	0.01	75	75	4.8
ZE-290A[a]											

(a) Not examined.

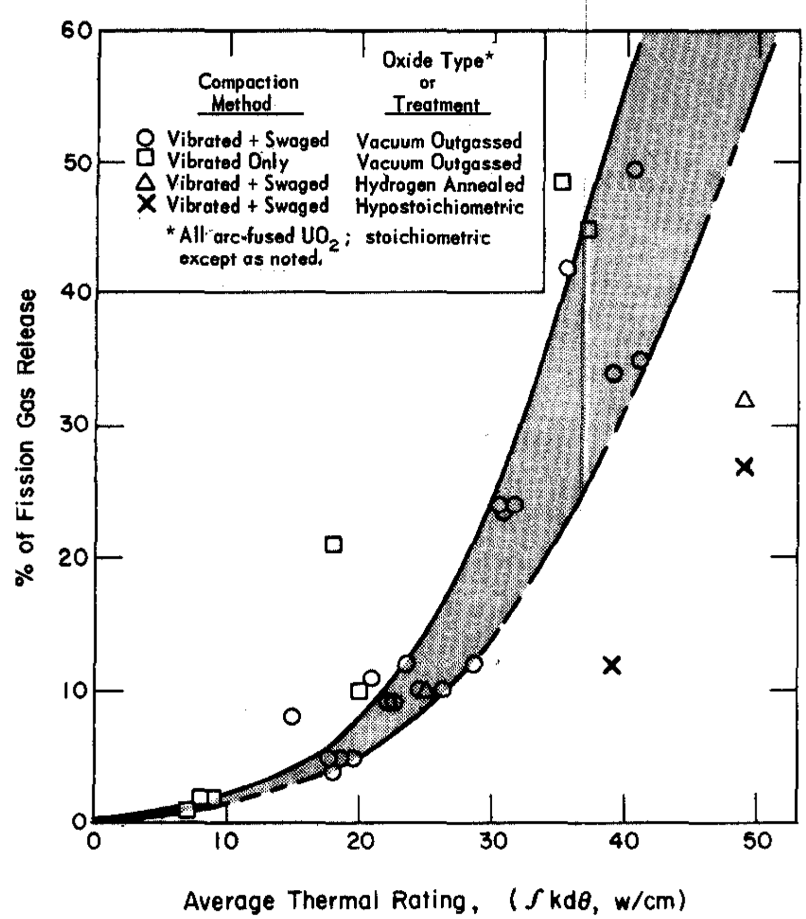

FIG. 6 FISSION GAS RELEASE vs. THERMAL RATING IN SWAGE-COMPACTED AND IN VIBRATORY-COMPACTED UO_2 TUBES

TABLE XII

Free Nitrogen Gas in Irradiated UO_2 Fuel Elements

Pretreatment of Fused UO_2 [a]		Number of Tubes	Peak $\int k d\theta$, watts/cm		Free Nitrogen Released During Irradiation, cc at STP/kg of UO_2	
			Mean	Range	Mean	Range
Vacuum Outgassed						
Time, hr	Avg Temp, °C					
3/4-1	1000-1100	11	19	11-25	55	0.2-101
4	1300-1400	10	29	21-39	15	5-25
4	1500-1600	18	31	4-55	6	0.2-23
Hydrogen Treated						
4	1300	1	52	-	1.2	-
12	1750	2	38	32-45	0.14	0.13-0.16
Hypostoichiometric ($UO_{1.98}$)						
No thermal treatment		3	39	18-54	0.04	0.03-0.05

(a) Oxygen-to-uranium ratio (O/U) = 2.00 to 2.02 unless otherwise shown.

DIMENSIONAL CHANGES

The average changes in dimensions of the irradiated tubes were acceptably small except where the outer sheaths wrinkled, or where melting was extensive in the central part of the core. The average changes in outside diameter, wall thickness, and volume of the base-case tubes are shown in Tables XIII through XV. Essentially no change in dimensions occurred during irradiation of tubes of the reference design that operated at the highest power levels in the SOT-6, SOT-8, and SOT-9 tests. The average changes in tubes that did not undergo wrinkling or central melting ranged from +6 to -3 mils for the outer diameters and +3 to -3 mils for the wall thicknesses. Variations of ±3 mils are believed to result primarily from scatter in the

TABLE XIII

Dimensional and Volume Changes of Irradiated UO_2 Tubes in SOT-1 Test

(Assemblies SOT-1-2 and SOT-1-3)

Tube No.	Average Dimensional Change, inch: Outer Diameter	Average Dimensional Change, inch: Wall Thickness	Volume Change, % of Preirradiated Core Volume
Assembly SOT-1-2			
ZE-222E[a]	+0.004	Not determined	Not determined
Assembly SOT-1-3			
ZE-232F	+0.001	+0.002	-0.4
ZE-225A	0.000	0.000	-0.8
ZE-228D	-0.001	+0.001	-0.4
ZE-225E	+0.002	+0.001	-1.2
ZE-228G	0.000	+0.002	0.0
ZE-222G	0.000	+0.001	-1.2
ZE-228B	0.000	+0.002	+0.4

(a) Only tube measured in Assembly SOT-1-2.

TABLE XIV

Dimensional and Volume Changes of Irradiated UO_2 Tubes in SOT-2 Test

(Assemblies SOT-2-2 and SOT-2-3)

Tube No.	Average Dimensional Change, inch: Outer Diameter	Average Dimensional Change, inch: Wall Thickness	Volume Change, % of Preirradiated Core Volume
Assembly SOT-2-2			
Z-257C	-0.001	+0.001	-0.3
Z-250B	0.000	0.000	+0.1
Z-256A	+0.002	+0.001	-0.4
Z-251A	-0.014(a) +0.058(b)	-0.006 -	-2.4
Z-251C	-0.054(a) +0.015(b)	-0.032 -	-8.7
Z-255B	+0.001	0.000	-0.9
Z-257B	-0.001	0.000	-1.2
Z-252C	0.000	0.000	-0.4
Assembly SOT-2-3			
Z-254A	+0.001	+0.003	0.0
Z-251B	+0.001	0.000	-0.4
Z-256B	+0.001	+0.001	-0.3
Z-252B	-0.044(a) +0.076(b)	-0.024 -	-4.5
Z-254B	+0.002	+0.001	0.0
Z-253C	-0.042(a) +0.089(b)	-0.016 -	Not determined
Z-257A	-0.001	0.000	-1.3
Z-253B	-0.001	-0.001	-1.0

(a) Over uniform section of tube.
(b) At crest of ridge formed by collapse of outer sheath.

TABLE XV

Dimensional and Volume Changes of Irradiated UO_2 Tubes in SOT-5 and SOT-7 Tests

(Assemblies SOT-5-2 and SOT-7-2)

Tube No.	Average Dimensional Change, inch: Outer Diameter	Average Dimensional Change, inch: Wall Thickness	Volume Change, % of Preirradiated Core Volume
Assembly SOT-5-2			
Z-262A	0.000	0.000	-0.7
Z-260C	+0.002	+0.002	-0.2
Z-259C	+0.006	+0.003	+0.3
Z-259D	+0.001	+0.002	-0.8
Z-261D(a)	+0.002(c) +0.034(d)	-0.003 -	-2.1
Z-261B	-0.003	-0.002	-1.5
Z-262B	-0.001	-0.001	-1.0
Assembly SOT-7-2			
Z-265C	+0.001	+0.001	-0.3
Z-261C	-0.003	0.000	-0.5
Z-260B	0.000	+0.001	-0.2
ZE-266C(b)	+0.007	+0.005	+1.2
ZE-266A(b)	+0.028	+0.012	+4.0
Z-264A(b)	+0.006	+0.003	+0.5
Z-265B	-0.002	-0.002	-0.6

(a) Partial collapse of the outer sheath occurred at the end of this tube where an area of low core density is believed to have inadvertently occurred during fabrication.
(b) Center melting occurred during irradiation.
(c) Over uniform section of core.
(d) At crest of ridge formed by collapse of outer sheath.

measurements and represent limits of the reliability of the data. For tubes that developed wrinkles in the outer sheath, the diameters at the crest of the associated ridge increased 19 to 105 mils; away from the ridge in the same region, the outer diameters decreased 14 to 54 mils.

In contrast to small decreases in volume generally observed for tubes irradiated at lower thermal ratings, volumes increased for tubes that operated with molten centers. Tube ZE-266A, irradiated at a peak thermal rating of 68 watts/cm, increased 4% in volume; the outer sheath of this element was bulged over its lower half and exhibited a maximum residual strain of 3% (76 mils) without rupture. Tube ZE-266C, operated at an average peak of 50 watts/cm and a maximum peak of 66 watts/cm, increased 1.2% in volume. Both increases are believed to result from the volume increase of UO_2 on melting.

Average changes in length calculated from pre- and post-irradiation measurements varied from -30 mils to +55 mils; however, this is believed to represent scatter in the data rather than actual changes in length.

CORE MICROSCOPY

The changes in compacted powder cores during irradiation were investigated to develop an understanding of the core temperatures developed during irradiation. Knowledge of the effect of thermal rating on core structure is helpful in predicting core behavior, e.g., gas release, plasticity, and approach to melting. The results of micrographic studies to relate core structural changes to thermal rating are given below.

The structure of the powder cores was modified during irradiation; the extent of the modification increased as the thermal rating ($\int k d\theta$) increased (see Figures 7 through 13). The gross appearance and state of coherence of as-cut sections of the cores can be seen in Figure 7. Greater detail of the core structure is shown in the mounted-and-polished sections of Figure 8.

The extent of interparticle sintering increased as the thermal rating increased to about 20 watts/cm. For example, unirradiated vibratory-compacted cores were easily emptied from the tube, but during irradiation, even below 5 watts/cm, sintering was sufficient to hold the core in place. Below 10 watts/cm, the interparticle sintering was weak as evidenced by loss of urania particles during sectioning; this loss did not occur at higher thermal ratings. At 15-20 watts/cm, the core was sintered enough to crack in the cut section (Figure 8b); fallout during cutting occurred only in the cooler regions near the sheath.

Grain growth began at ~25 watts/cm for vibratory-compacted cores and at ~30 watts/cm for swage-compacted cores (Figures 8b and 8d). At 35-40 watts/cm, nearly half of the core had undergone grain growth (Figure 8e). Above 50 watts/cm, columnar grain growth was so extensive that the original particle size distribution was no longer evident (Figure 8f).

Subgrains and small irregular grains that formed in a swage-compacted element irradiated at a peak $\int k d\theta$ of 32 watts/cm are shown in Figure 9. A few lenticular voids can be seen, but the thermal gradient at this location was probably too low to produce significant void migration with the resulting formation of columnar grains.

Columnar grain growth was extensive in a swage-compacted element irradiated at a peak $\int k d\theta$ of 39 watts/cm (see Figure 10). Approximately midway between the edge and center of the core, lenticular voids have formed and started to move up the thermal gradient leaving small columnar grains in their wakes. Most of these small grains are unstable, and at higher temperatures the boundaries are believed to collapse upon the void (see Figure 10).

At the thermal center, a large void has formed that divides the core into two nearly equal parts. Adjacent to the central void are many voids, some nearly spherical, that are randomly distributed within grains and on boundaries. These voids may be anchored at these sites or may be migrating very slowly because of the small thermal gradient in this region. The voids can grow

Tube	Thermal Rating watts/cm Avg	Max
a. Tube Z-251B (Vibrated)	10	14
b. Tube Z-256B (Vibrated + Swaged)	18	24
c. Tube Z-257A (Vibrated + Swaged)	32	36

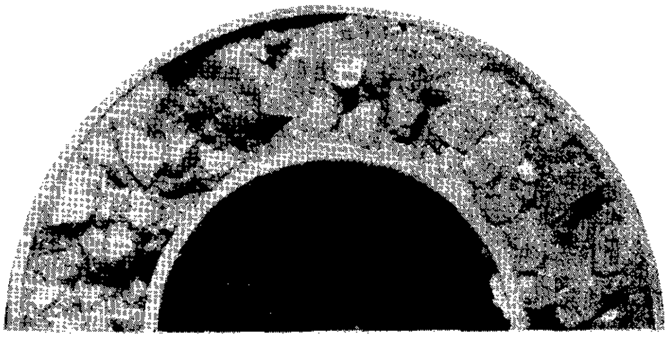

NEG. 52680

a. Tube Z-251B (Vibrated)

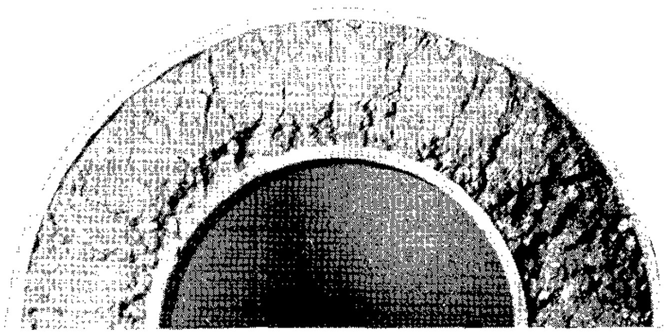

NEG. 52685

b. Tube Z-256B (Vibrated + Swaged)

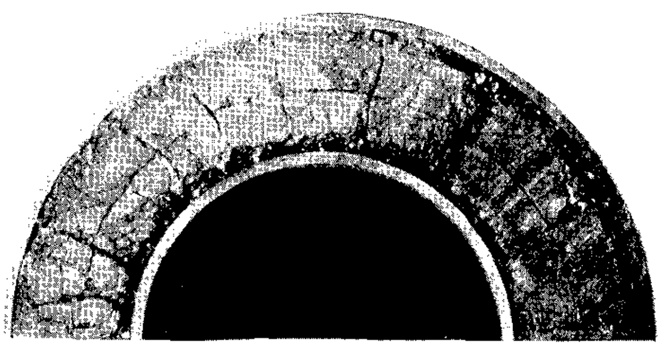

NEG. 52705

c. Tube Z-257A (Vibrated + Swaged)

FIG. 7 EFFECT OF THERMAL RATING ON CORE STRUCTURE

Thermal Rating, watts / cm

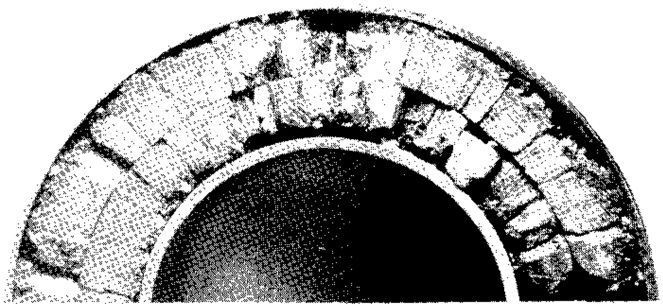

NEG. 52663

Tube	Avg	Max
d. Tube Z-255B (Vibrated + Swaged)	41	46

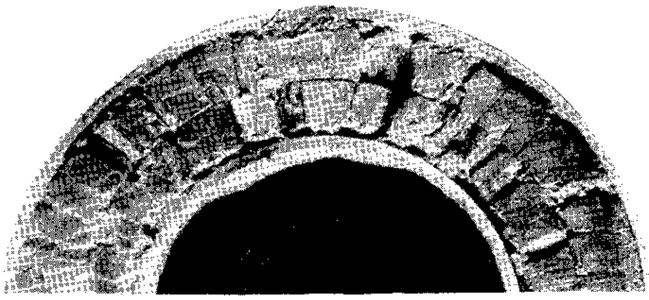

NEG. 52662

Tube	Avg	Max
e. Tube Z-251C (Vibrated)	45	50

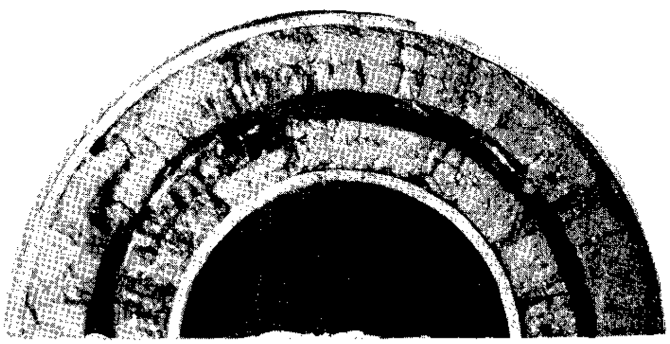

NEG. 59291

Tube	Avg	Max
f. Tube ZE-266A (Vibrated + Swaged)	63	67

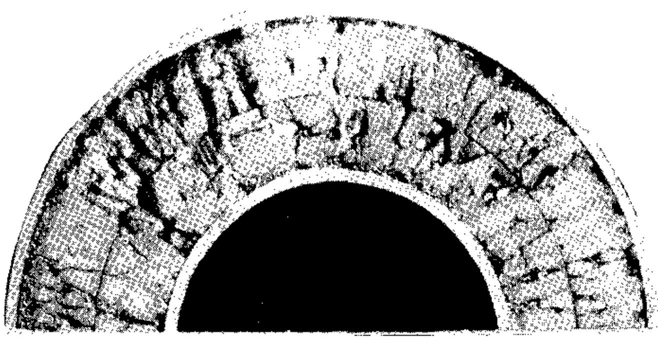

NEG. 59290

Tube	Avg	Max
g. Tube ZE-266A (Vibrated + Swaged)	65	68

OF AS-CUT SECTIONS OF IRRADIATED UO_2 TUBES ($\sim$2X)

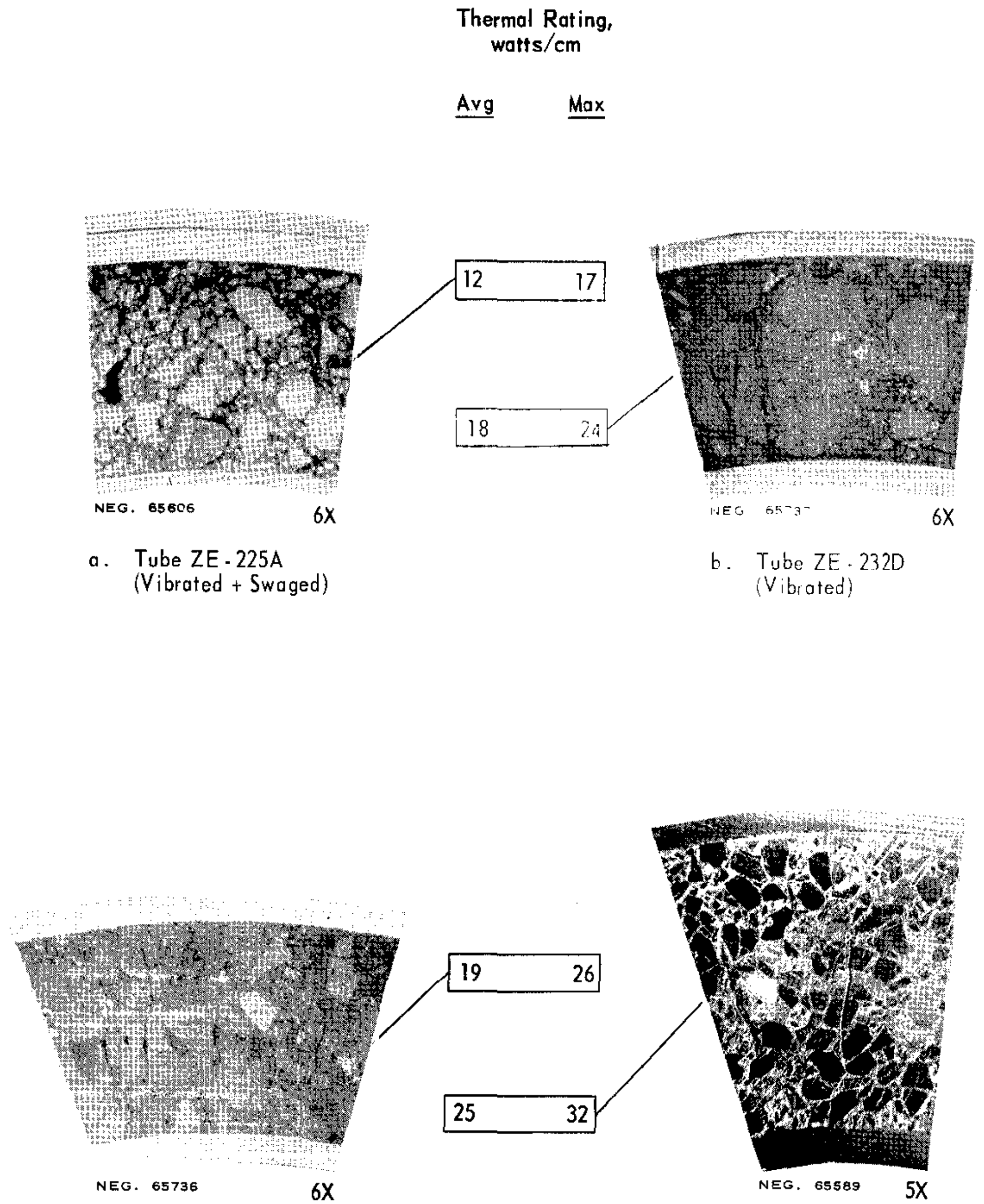

a. Tube ZE-225A (Vibrated + Swaged)

b. Tube ZE-232D (Vibrated)

c. Tube ZE-222E (Vibrated + Swaged)

d. Tube Z-256B (Vibrated + Swaged)

FIG. 8 EFFECT OF THERMAL RATING ON CORE STRUCTURE OF

Thermal Rating,
watts/cm

Avg	Max
36	39
49	55
66	68

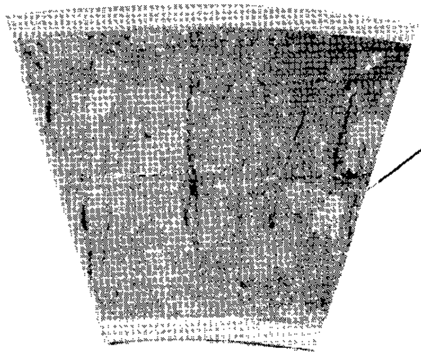

NEG. 65729 6X

e. Tube ZE-280C
(Vibrated + Swaged)

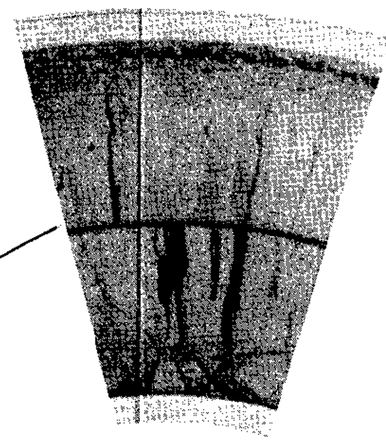

NEG. 66022 5X

f. Tube Z-259D
(Vibrated + Swaged)

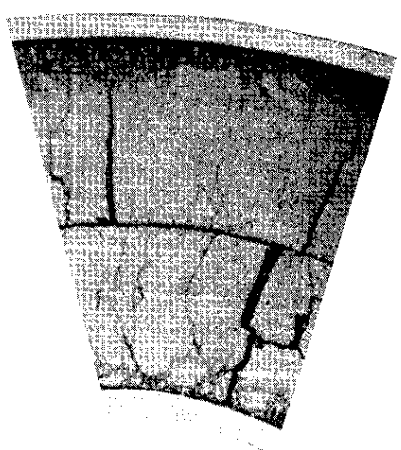

NEG. 62243 5X

g. Tube ZE-266A
(Vibrated + Swaged)

GROUND-AND-POLISHED SECTIONS OF IRRADIATED UO_2 TUBES

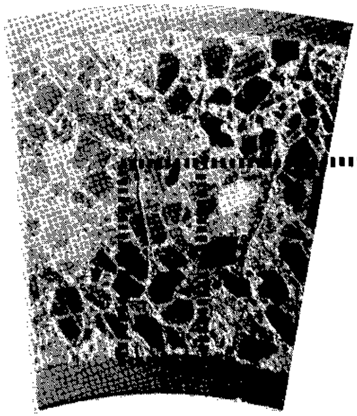

NEG. 65689 4X

a. Section of tube Z-2563, which operated at $\int kd\theta = 25$ avg, 32 max watts/cm.

NEG. 65686 b. 35X

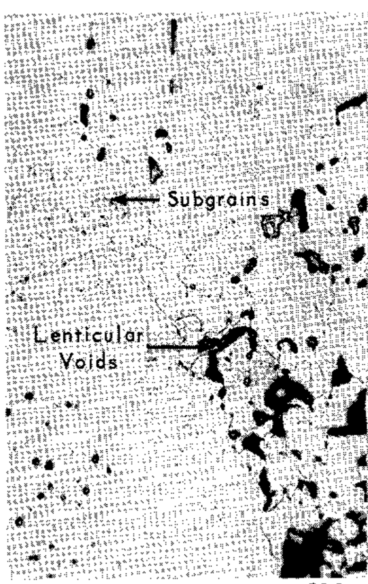

NEG. 65596 210X

c. Evidences of internal readjustments are shown by formation of subgrams, small irregular grains, and lenticular voids.

FIG. 9 SINTERING AND INCIPIENT GRAIN FORMATION IN SWAGE-COMPACTED UO_2 CORE

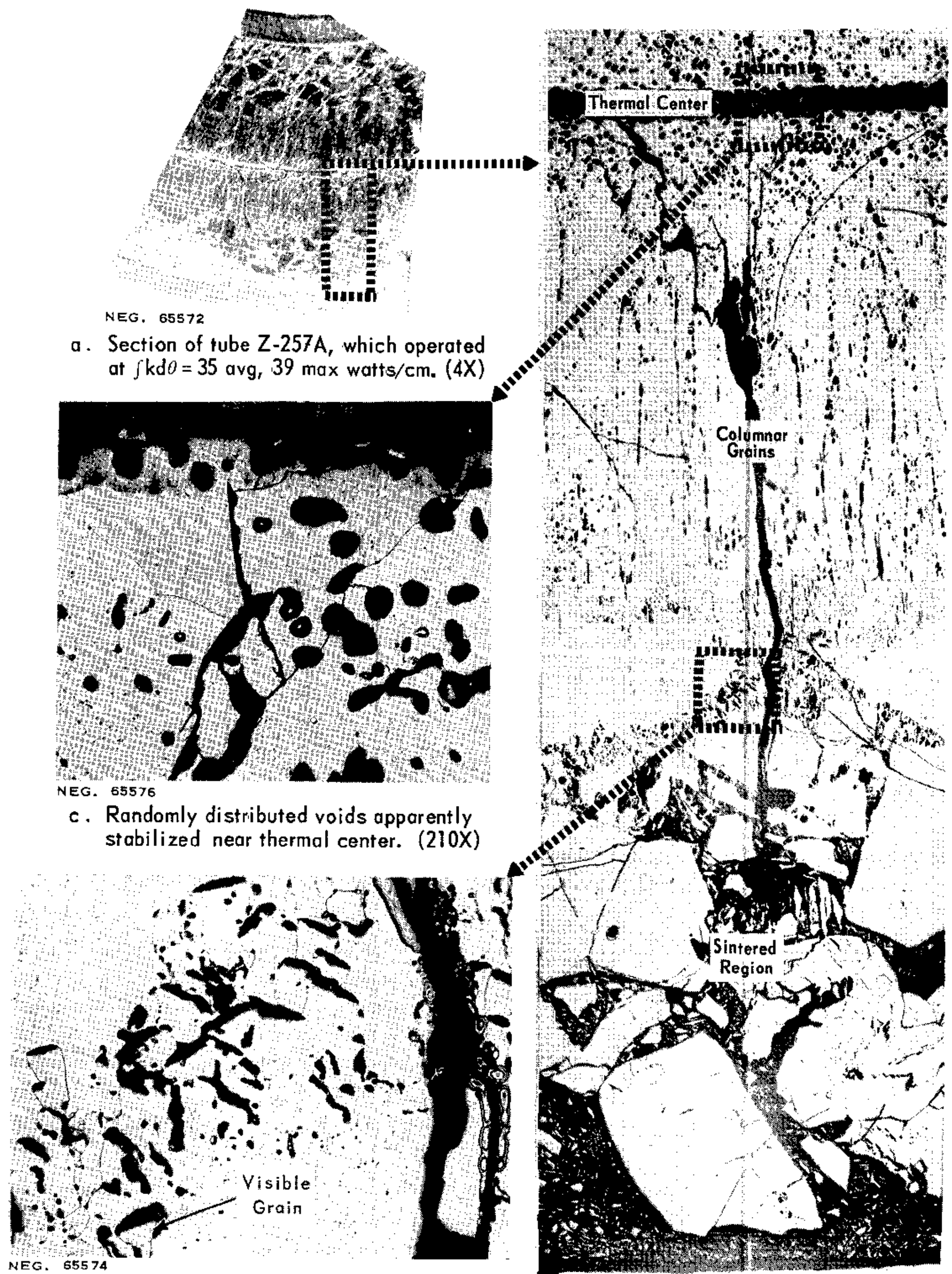

a. Section of tube Z-257A, which operated at $\int kd\theta = 35$ avg, 39 max watts/cm. (4X)

b.

c. Randomly distributed voids apparently stabilized near thermal center. (210X)

d. Lenticular voids that migrated short distances to form small columnar grains. (210X)

FIG. 10 COLUMNAR GRAINS IN A SWAGE-COMPACTED UO_2 CORE

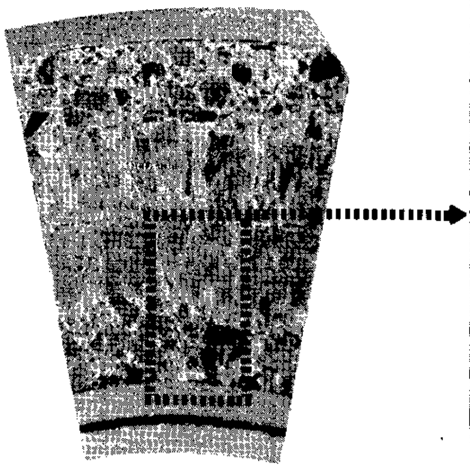

a. Section of tube Z-257A, which operated at $\int kd\theta = 29$ avg, 34 max, watts/cm.

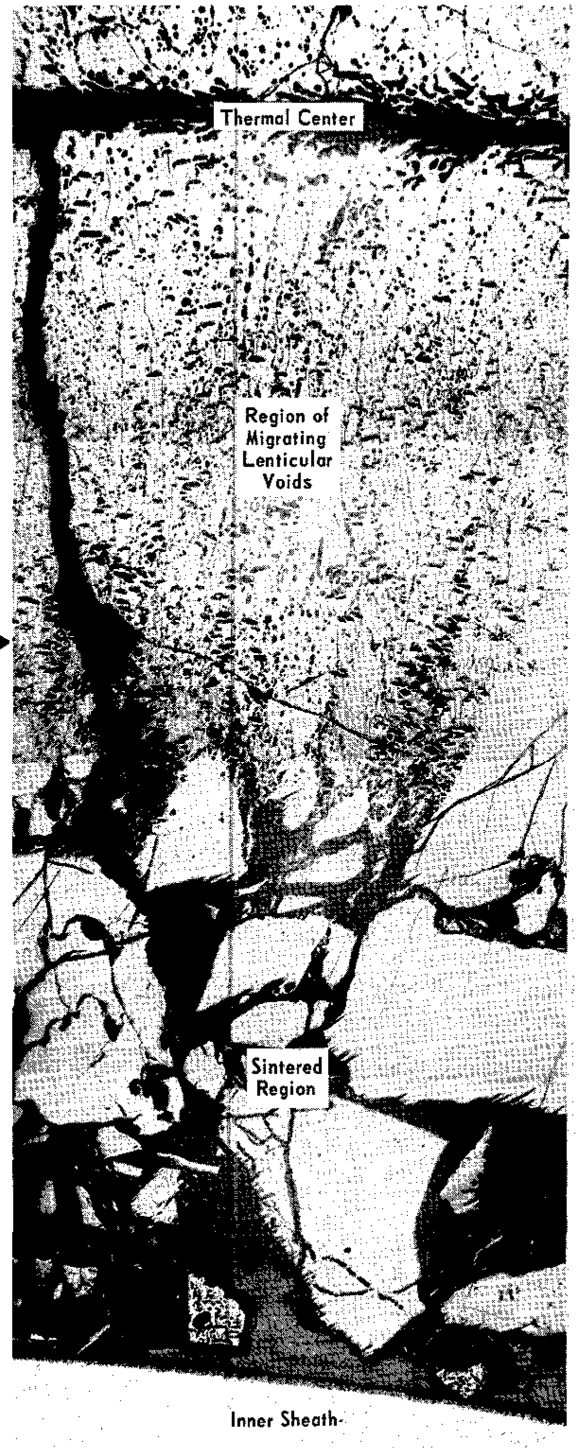

b. 35X

FIG. 11 MIGRATION OF LENTICULAR VOIDS AND FORMATION OF SMALL COLUMNAR GRAINS IN UO_2 CORE. (Core section that operated at avg/max $\int kd\theta$ of 29/34 watts/cm from same tube as Fig. 10.)

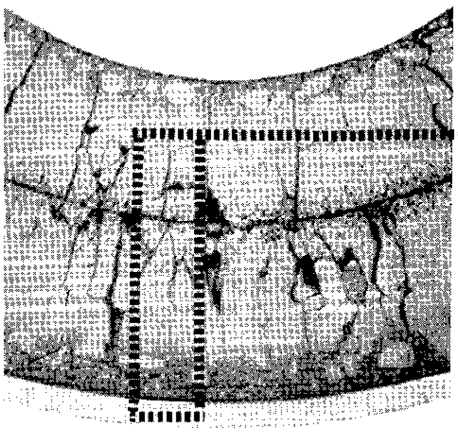

NEG. 66007 4X

a. Section of tube ZE-266A, which operated at $\int kd\theta = 63$ avg, 67 max, watts/cm.

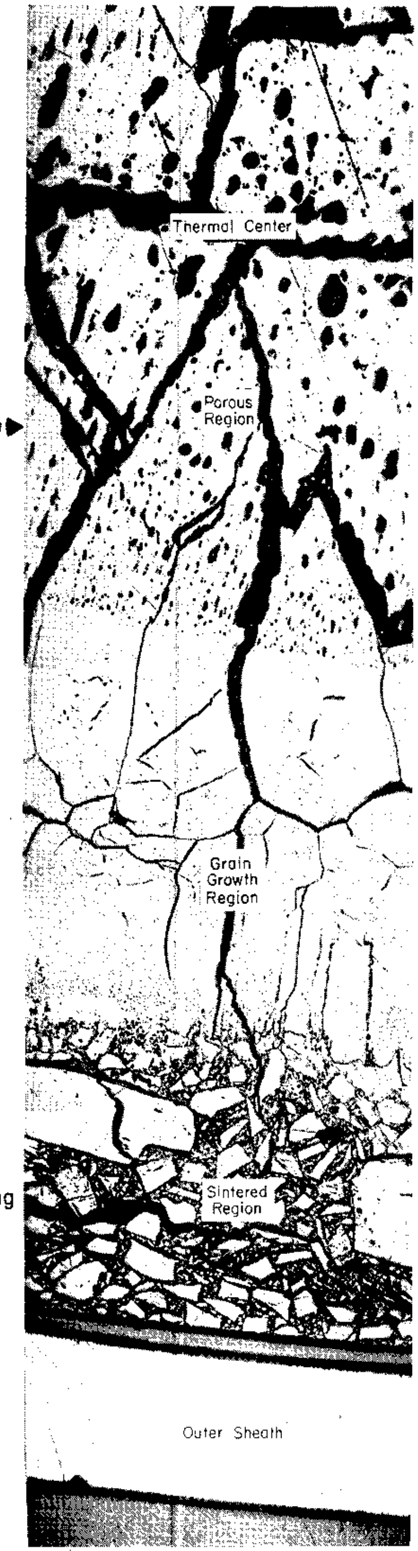

16X

b. Large porous zone is believed to define a region of central melting

FIG. 12 STRUCTURE OF UO_2 CORE AFTER IRRADIATION AT HIGH THERMAL RATINGS

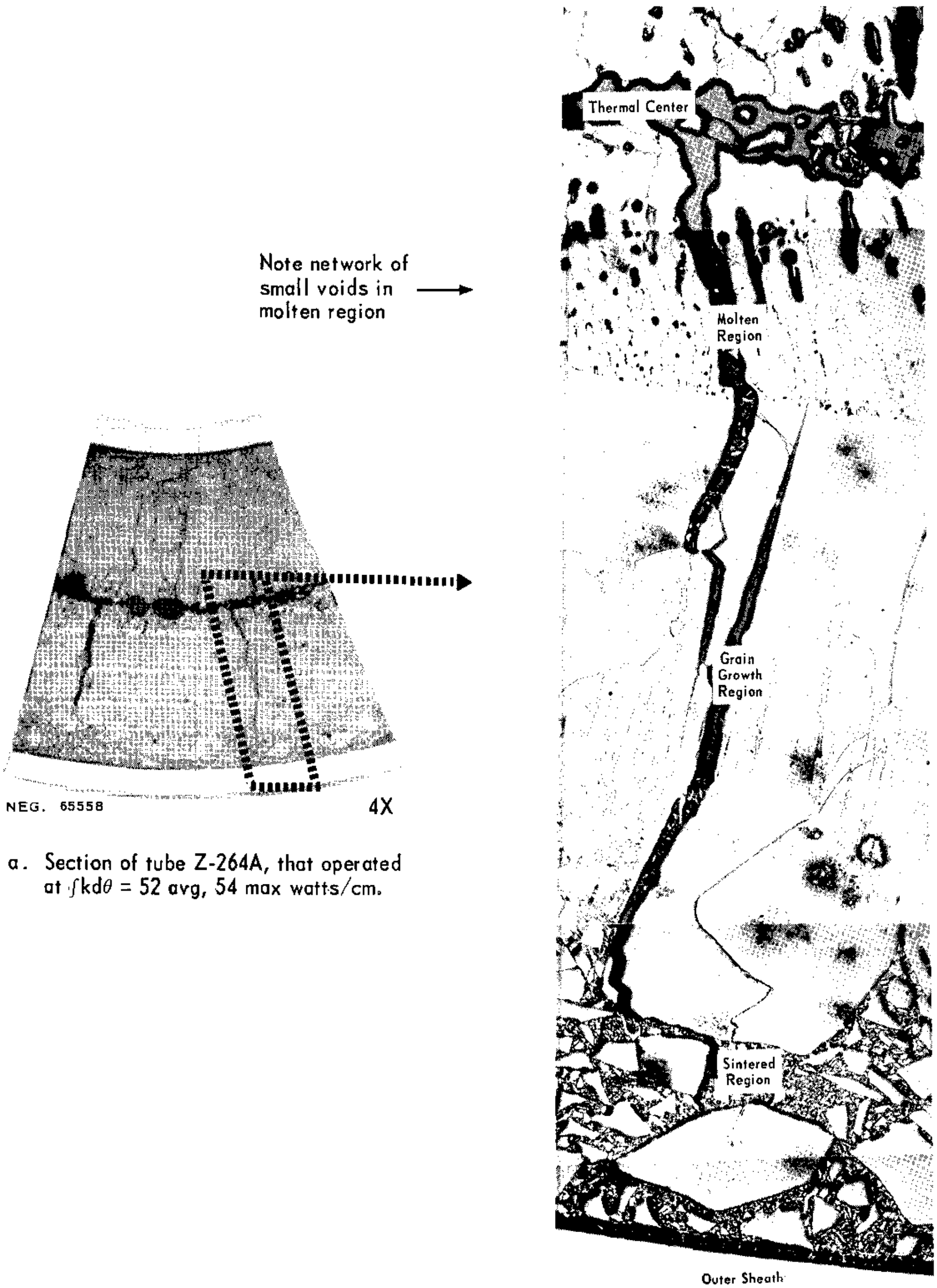

a. Section of tube Z-264A, that operated at $\int k d\theta$ = 52 avg, 54 max watts/cm.

b. 30X

FIG. 13 CORE STRUCTURE SHOWING NETWORK OF SMALL VOIDS IN POROUS ZONE by diffusion of gases from the UO_2 matrix, but probably most of these gases diffuse along grain boundaries to the central void. The region of core containing spherical voids is separated from the region containing lenticular voids by a region of large columnar grains (Figure 10). These grains are probably the combined result of previous void migration followed by grain growth at an earlier time in the irradiation.

An earlier stage of columnar grain formation in the same element is shown in Figure 11 for a section that operated at a lower thermal rating than the section shown in Figure 10. In the portion at lower thermal rating, a dense population of lenticular voids extends from about the mid-radius position to the thermal center.

Central melting began at 55 to 60 watts/cm. Two cross sections from Tube ZE-266A show an annular shrinkage cavity (about 1 inch long) near the top of the tube (Figure 7f), and a solid cross section over the remainder of the core (Figure 7g). The porous zone that extends about a third of the way from the central void to the surface of the core (Figures 8g and 12) provides additional evidence of melting in this element. Central porous zones containing both large isolated voids and small voids distributed on a substructure network have been identified by HAPO[14] as regions that were molten during irradiation. The substructure of small voids is clearly evident in the molten region indicated in Figure 13.

SHEATH METALLOGRAPHY

Sheath specimens were examined metallographically with particular attention to the incidence and distribution of zirconium hydride because of the known embrittlement that can result when hydride platelets are present in large amounts or in unfavorable distributions, for example, in strongly radial orientations. The hydride platelets tended to concentrate at the coolant side of the Zircaloy-2 sheathing, and a thin layer of surface oxide was observed on the core side of most sheath specimens. However, neither hydride nor oxide formation appears likely to impair the serviceability of the cladding. The regions of concentrated hydride were confined to within about 0.007 inch of the surface. In the outer sheaths the hydride platelets were oriented circumferentially, whereas in the inner sheaths, the hydride platelets were generally oriented randomly with only a slight preference for radial orientation. The heaviest concentrations of hydride were in the Zircaloy-2 sheaths of the large-size and intermediate-size tubes, SOT-8 and SOT-6 tests, irradiated for 88 and 160 days, respectively (Figures 14 and 15).

Sheaths fabricated from low-nickel Zircaloy-2 exhibited very little zirconium hydride after irradiation (Figure 16). Test pieces from SOT-1-2 (irradiated for 416 days) exhibited trace-to-light concentrations of fine hydride platelets similar to the hydride concentrations reported earlier on like tubes after an irradiation of much shorter duration in a SRP production reactor.[15,16]

Hydride orientations produced in the HWCTR tests were different from those in the earlier SRP tests. In the elements irradiated under 1000-1200 psi coolant pressure, the pressure within the tube was always less than the coolant pressure. The resulting sheath stresses led to circumferentially oriented platelets in the outer sheaths and random or sometimes radially oriented platelets in the inner sheaths. In the earlier SRP irradiation of short duration, the internal pressure within the tubes exceeded the coolant pressure, and the resultant stresses in the sheaths led to random or radially oriented platelets in the outer sheaths and predominantly circumferential platelet orientation in the inner sheaths.

In the inner sheath tubing used in the SOT-2 tests, an undesirable radial orientation of hydride platelets occurred as a result of fabrication. These sheaths were fabricated from extruded-and-drawn Zircaloy tubing that was cold sized in a final sinking operation. The radial hydride platelets formed when the fuel tube was autoclaved in steam and persisted throughout the irradiation; however, cladding did not rupture in these sheaths. By annealing the cold-worked tubing, radial platelets were eliminated and a random distribution of platelets was produced (Figure 17).

Outer Sheath

Coolant

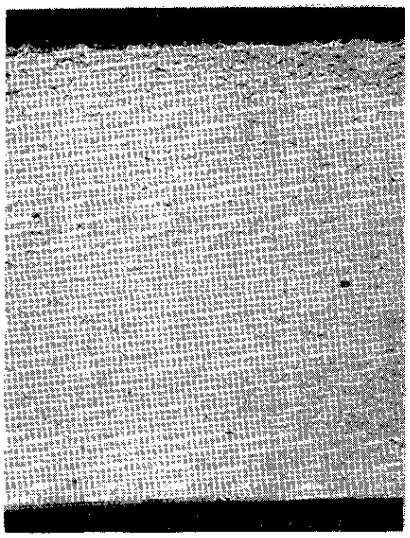

NEG. 65743

Core

Inner Sheath

Core

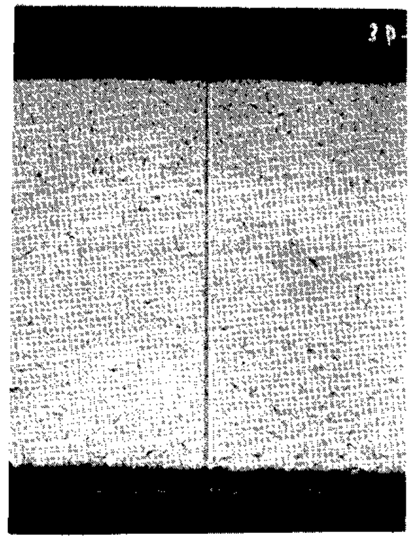

NEG. 65744

Coolant

As-polished sections, showing hydride distribution across the sheaths. (75X)

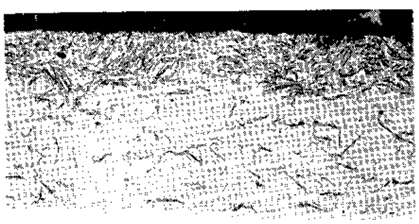

NEG. 65727

NEG. 65740

Etched sections, showing hydride platelets nearest the coolant. Note that in outer sheath platelets tend to be in circumferential plane; in inner sheath, platelets are random or radial. (250X)

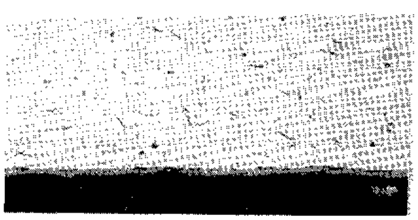

NEG. 65730

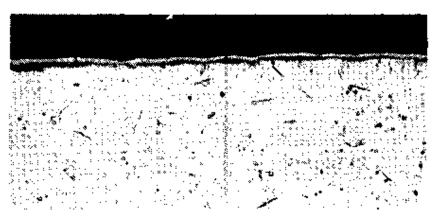

NEG. 65733

Etched sections, showing hydride platelets nearest UO_2 core. Note layer of ZrO_2 at interface. (250X)

FIG. 14 DISTRIBUTION OF ZIRCONIUM HYDRIDE IN ZIRCALOY-2 SHEATHS (3.7-INCH-DIAMETER REFERENCE DESIGN) Transverse section of Tube ZE-297B, SOT-8-3, irradiated 88 days.

Outer Sheath
Coolant

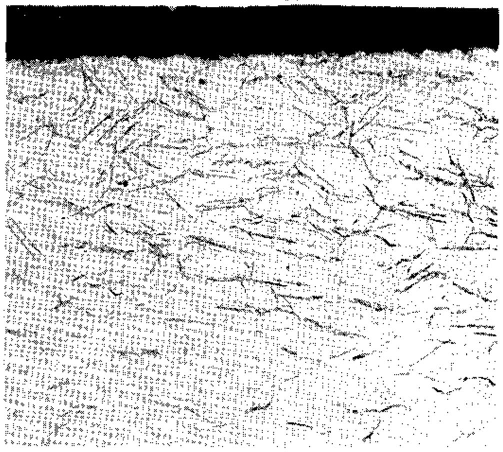

NEG. 65742

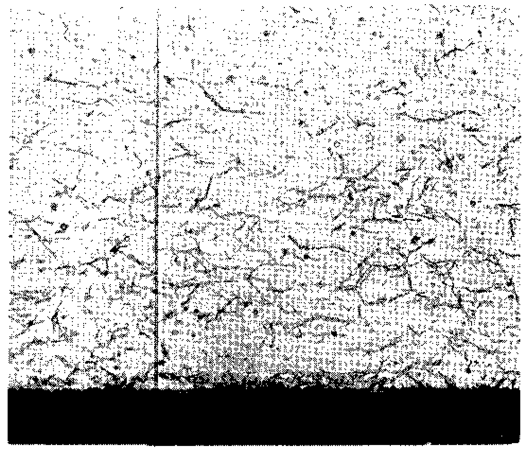

NEG. 65739

Inner Sheath
Coolant

Etched sections, showing hydride platelets nearest coolant. Note strong tendency for preferred circumferential orientations in the outer sheath tubing. (250X)

NEG. 65741

Core

Core

NEG. 65738

Etched sections, showing hydride platelets nearest core. Note that platelets in outer sheath are circumferential; those of inner sheath are largely radial. Layer of ZrO_2 is also visible on inner sheath specimen (250X)

FIG. 15 DISTRIBUTION OF ZIRCONIUM HYDRIDE IN ZIRCALOY-2 SHEATHS (2.5-INCH-DIAMETER REFERENCE DESIGN) Transverse sections of Tube Z-278C, SOT-6-2, irradiated 160 days.

Outer Sheath

Coolant

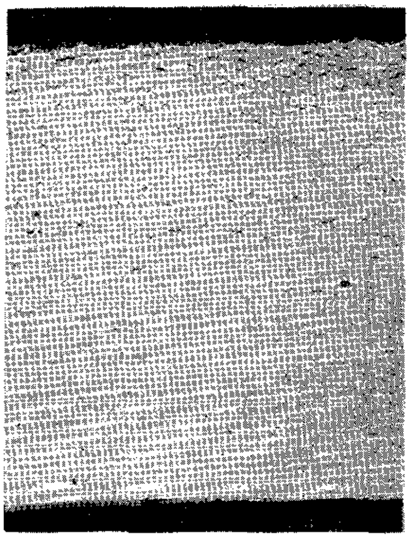

NEG. 65743

Core

Inner Sheath

Core

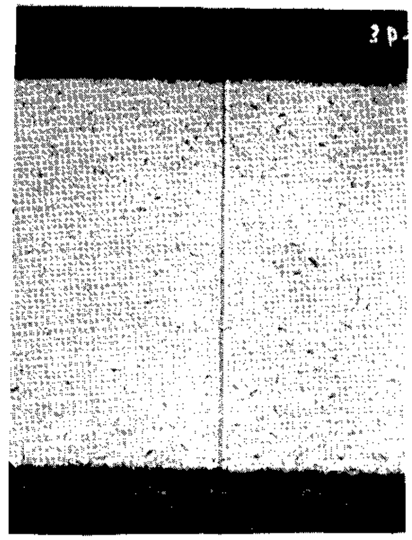

NEG. 65744

Coolant

As-polished sections, showing hydride distribution across the sheaths. (75X)

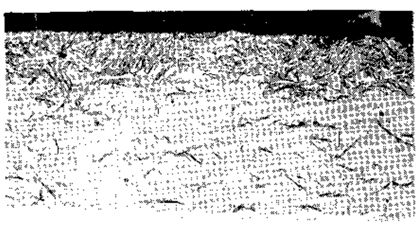

NEG. 65727

NEG. 65740

Etched sections, showing hydride platelets nearest the coolant. Note that in outer sheath platelets tend to be in circumferential plane; in inner sheath, platelets are random or radial. (250X)

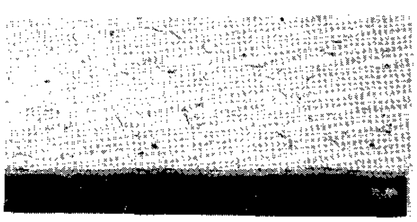

NEG. 65730

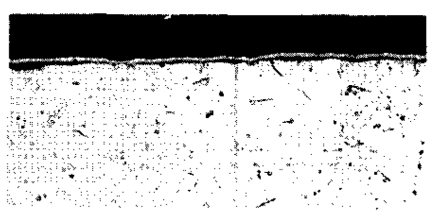

NEG. 65733

Etched sections, showing hydride platelets nearest UO_2 core. Note layer of ZrO_2 at interface. (250X)

FIG. 14 DISTRIBUTION OF ZIRCONIUM HYDRIDE IN ZIRCALOY-2 SHEATHS (3.7-INCH-DIAMETER REFERENCE DESIGN) Transverse section of Tube ZE-297B, SOT-8-3, irradiated 88 days.

Outer Sheath

Coolant

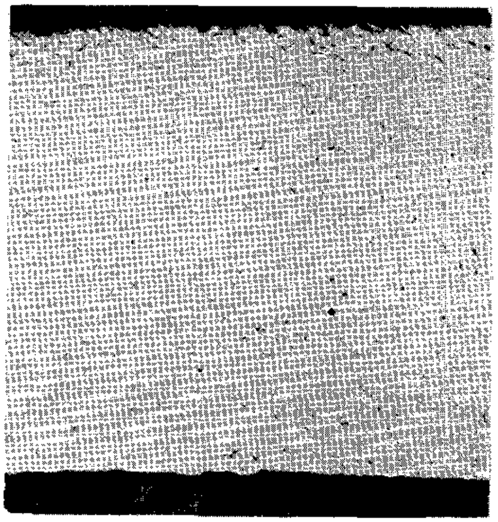

NEG. 65735

Core

Inner Sheath

Core

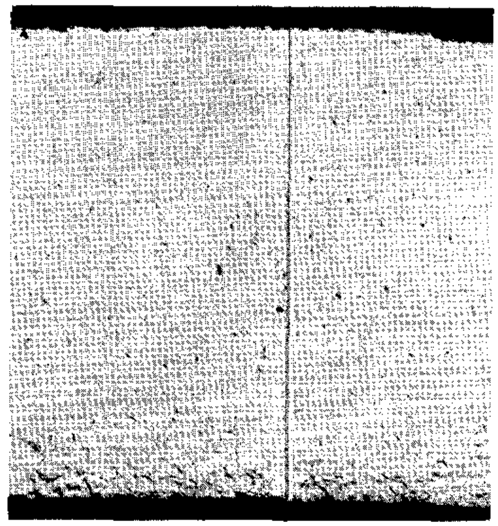

NEG. 65734

Coolant

As - polished sections, (75X)

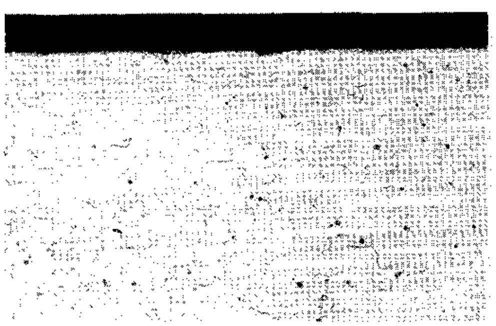

NEG. 65731

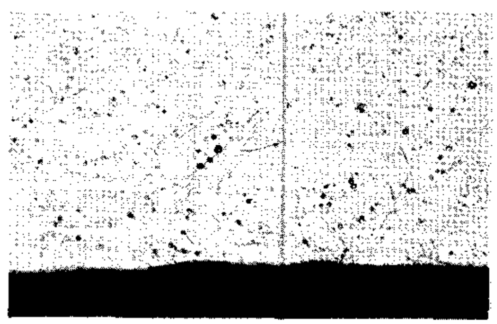

NEG. 65732

Etched sections showing light concentrations of fine platelets nearest the coolant. (250X)

FIG. 16 DISTRIBUTION OF ZIRCONIUM HYDRIDE IN LOW-NICKEL ZIRCALOY-2 SHEATHS (2.1-INCH-DIAMETER BASE-CASE DESIGN) Transverse sections of Tube ZE-22E, SOT-1-2, irradiated 416 days.

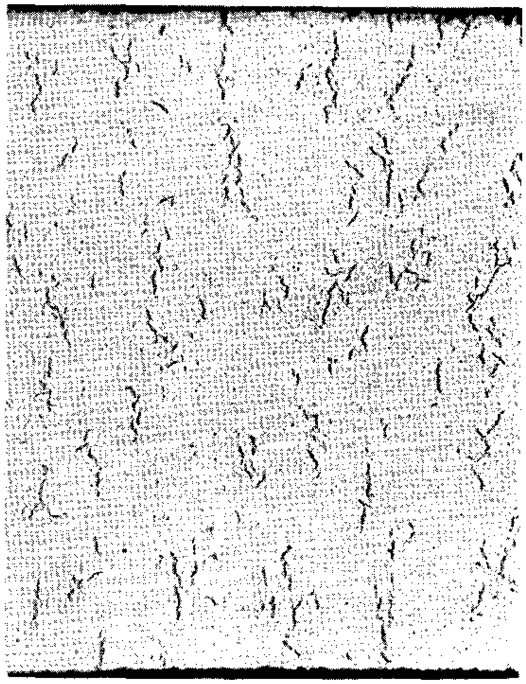

NEG. 51276-1 100X

a. Radial distribution of hydrides, typical of tubing used as inner sheaths in SOT-2 elements in as-cold reduced condition.

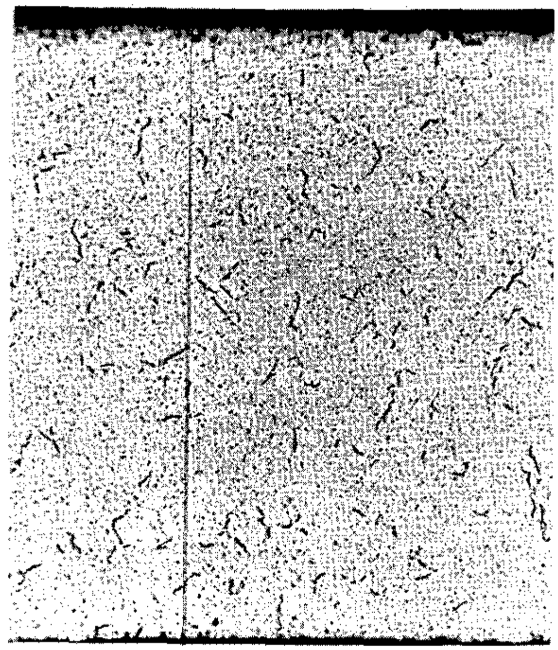

NEG. 51280-2B 100X

b. Random distribution of hydrides, typical of similar tubing in cold reduced-and-annealed condition.

FIG. 17 DIFFERENT HYDRIDE ORIENTATIONS FOUND IN ZIRCALOY-2 TUBING AFTER AUTOCLAVING IN STEAM FOR 48 HOURS AT 750°F.

SHEATH FAILURES

In the HWCTR irradiation program, eleven of the 97 UO_2 elements failed during testing; in nine of these failures, the integrity of the Zircaloy sheath was lost, and either fission products leaked into the coolant, or the heavy water coolant leaked into the slug. In no case was there any extensive physical damage or appreciable release of UO_2. Four failures caused by wrinkling of the outer sheath were discussed in an earlier section of this report; sheath cracks occurred at the apex of the wrinkle in two of these tubes and released fission product gases to the coolant. The remaining sheath failures are discussed in the following paragraphs.

Sheath Failures Caused by Mechanical Vibration

Two long oxide tubes failed during operation at moderate thermal ratings (about 25 watts/cm). Although these tubes were not examined, failures were probably due to sheath damage resulting from excessive vibration of the elements during irradiation. Companion elements irradiated at the same time exhibited severe mechanical wear in the form of deep grooves near the top of the tubes. Vibration was eliminated by redesign of the top fitting, and other long tubes were irradiated satisfactorily to peak exposures of 12,000 MWD/MTU.

Sheath Failure Caused by Faulty Weld Closure

One element in a column of short tubes failed during a power ascension after a short time in the reactor; the maximum exposure was only 30 MWD/MTU. The maximum thermal rating which was reached just prior to detection of the failure was ~20 watts/cm. Inspection of the assembly revealed that the failed tube was in the region of peak neutron flux; the visible evidence of failure was a ridge caused by collapse of the inner sheath. The other six tubes in the column were intact and undamaged.

In subsequent examination of the failed tube three leaks were found: one at the weld of a bottom vent hole, one at the circumferential weld of the inner sheath to the bottom end cap, and one at the crest of the longitudinal ridge that formed when the inner sheath collapsed. The hole at the vent seal resulted from inadequate sealing during fuel tube fabrication; this hole probably caused the failure. The other two holes probably resulted from deformation associated with collapse of the inner sheath or from interference between the collapsed sheath and inner housing tube during disassembly.

Examination of cross sections of the failed element indicated that the inner sheath collapsed after nuclear shutdown of the HWCTR. The UO_2 was mildly sintered - characteristic of normal operation at 15 to 20 watts/cm; there was no evidence of abnormally high core temperatures at the point of sheath collapse

(Figure 18). After the first indication of failure, the failed tube operated steadily at its peak rating for over an hour with little additional release of activity. If the first indication of failure coincided with collapse of the sheath, some grain growth should have occurred in the UO_2.

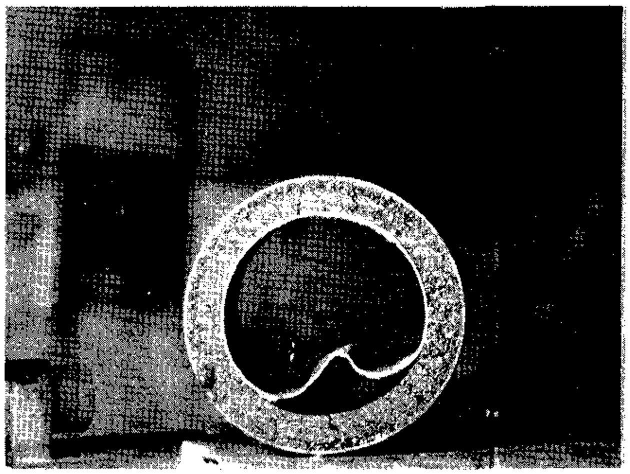

NEG. 59877 0.7X

NEG. 59878 7X

At Site of Collapse

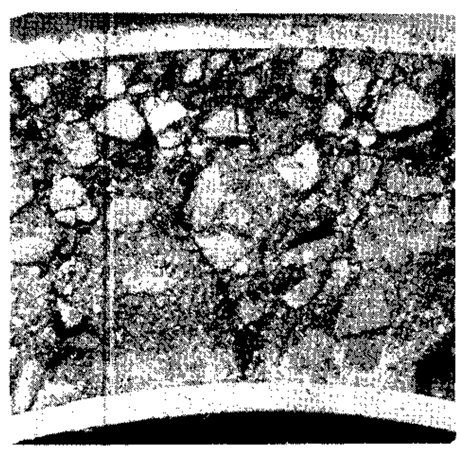

NEG. 59879 7X

Away From Site of Collapse

FIG. 18 SECTION OF FAILED TUBE SHOWING COLLAPSE OF INNER SHEATH AND MILD SINTERING OF UO_2 CORE

Sheath Failures Caused by Center Melting

Tube ZE-266A of the SOT-7-2 assembly, operating at an average peak thermal rating of 68 watts/cm, failed after an exposure of only 1100 MWD/MTU (see Table IV); subsequent examination revealed that central melting had occurred in three elements in this assembly. The tube was located in the peak flux position of the column. A hole about 0.05 inches in diameter was found in the inner sheath of this element over the upper void chamber, about 0.2 inch above the top end of the core. Destructive examination of this tube revealed a corresponding hole in the inner wall of the carbon steel void chamber; in addition, one of the small holes in the septum that served to admit gas from the core space to the void chamber was enlarged and some of the urania had entered the upper void chamber. From these observations, the intrusion of molten urania into the upper void chamber and/or into the small annular clearance between the chamber wall and the inner sheath probably caused the failure.

Known or Suspected Sheath Failures from Unknown Causes

During the HWCTR irradiation program three sheaths failed (or are suspected to have failed) for reasons that have not been adequately explained. The outer sheath of one of the SOT-5-2 tubes (Table IV) developed a very small hole and released fission products to the coolant. The gas content after irradiation of one tube each in the SOT-2-3 and SOT-7-2 assemblies included deuterium, presumably from an in-leakage of coolant (Tables VIII and IX).

Assembly SOT-5-2

The SOT-5-2 assembly was discharged from the reactor because of a signal of activity release, after a peak exposure of 1700 MWD/MTU at a peak thermal rating of 56 watts/cm. Although examination of the seven tubes from this assembly revealed no evidence of failure, Tube Z-259D irradiated in the region of peak neutron flux showed anomalous behavior during the release, measurement, and sampling of the gas in the slug. Because lower gas pressure was indicated by the McLeod gage than by the absolute manometer, a condensible vapor such as D_2O or H_2O was suspected. Analysis of the gas sample revealed that the primary component of the dry gas was D_2, with lesser quantities of HD and H_2, and with much less than the usual quantities of helium and xenon. All of these observations indicated that the slug had developed a leak while in the reactor. A small hole in the outer sheath was finally located by pressurizing the void space of the tube with argon, immersing the tube in water, and observing the slow escape of small bubbles.

A section of the sheath containing the defect was removed for metallographic examination. A small area of the inner surface of this section exhibited a white deposit, possibly zirconium oxide, in the vicinity of the defect. The section was ground, polished, and examined in succession until the defect was located. Although the cause and sequence of events leading to failure were not determined, the following information was obtained.

- The sheath was severely hydrided in the vicinity of the failure; the hydride began at the coolant surface and extended to more than halfway through the sheath.

- Several cracks extended from the coolant surface through the hydrided region. One of these connected with a crack which began at the inner surface of the sheath (Figure 19).

- The cracks that penetrated into the sheath from the inner surface contained an unknown material, possibly zirconium oxide. These cracks appeared to be randomly distributed opposite the hydrided region except that their size and frequency increased at locations where cracks that started at the coolant surface had penetrated the hydrided region.

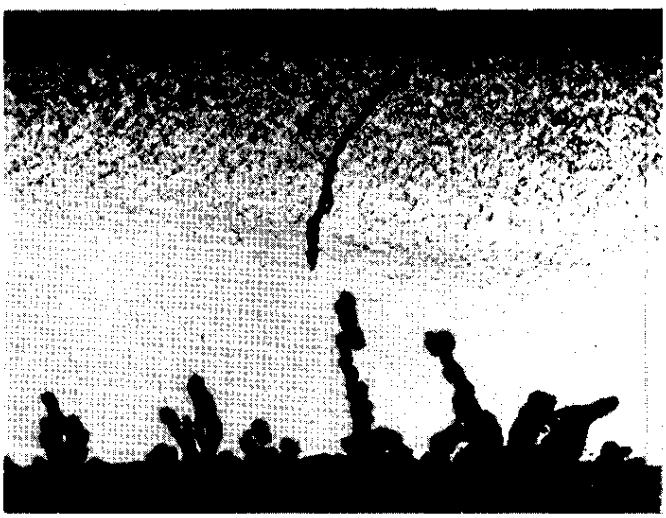

a. Sheath cracks meet within 0.003 inch of this section. Etched

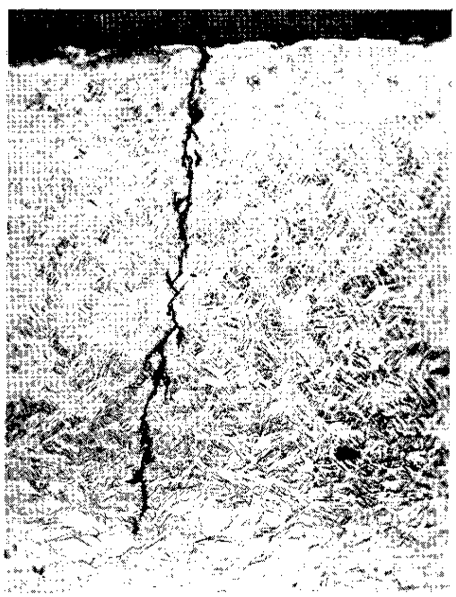

b. Crack 0.012 inch long extends through region of massive zirconium hydride. Sheath was penetrated within 0.03 inch of this section. Etched.

c. Crack 0.006 inch long extends into sheath from core interface and meets crack from coolant surface 0.008 inch from this section. Etched.

FIG. 19 MICROSTRUCTURE NEAR IN-PILE FAILURE IN OUTER SHEATH

- The structure of the Zircaloy sheath beneath the hydrided region was unchanged from the pre-irradiation condition except that the scattered hydride platelets had disappeared. All cracks in the sheath tubing were in the vicinity of the failure.

Assemblies SOT-2-3 and SOT-7-2

The SOT-2-3 and SOT-7-2 assemblies were discharged from the reactor because of activity release; the failed tubes in these assemblies were readily identified and examined as described in preceding sections; routine destructive examination of the remaining tubes revealed that one tube from each assembly contained deuterium.

Tube Z-254B (from SOT-2-3) contained 218 cc D_2/kg UO_2 (see Table VIII), equivalent to an internal pressure of 150 psi at room temperature. The coolant pressure (1200 psi) evidently caused leakage of D_2O into the tube through an undetermined sheath defect. The D_2O reacted with the Zircaloy sheathing or with impurities in the UO_2 to release deuterium; the small leak subsequently became plugged, presumably with corrosion products, so that at least part of the D_2 was unable to leak out of the tube when the tube was discharged from the reactor. This tube was pressure tested with helium at 57 psi for 26 hours as for the SOT-5-2 failure, but the location of this leak was not found.

The nature of the failure described above for Tube Z-254B presumably applies also to Tube Z-265C from the SOT-7-2 assembly (see Table IX). The gas sample from this tube contained D_2, HD, and H_2; however, the analyses were not completed until the tube had been sectioned; thus this tube was not pressure tested.

DISCUSSION

Test irradiations of Zircaloy-sheathed tubes of fused and compacted urania indicate that tubes fabricated by current techniques will operate satisfactorily in D_2O-cooled reactors at a peak $\int k d\theta$ of 30 watts/cm to exposures of 20,000 MWD/MTU. This prediction assumes that the fraction of fission gas released is independent of exposure over the range of interest. Preliminary computer calculations[17] show that, for D_2O-cooled reactors as large as 500 MWe, the overall cost penalty for the 30 watts/cm limit is only about 0.1 mill/kwh when compared with tubes operating at 55 watts/cm (the computed optimum rating).

A total of 138 urania tubes with Zircaloy sheathing were irradiated over a broad range of exposures and thermal ratings. The maximum exposure was 17,000 MWD/MTU, and the maximum thermal rating was 68 watts/cm. Problems revealed during these tests are discussed below.

OUTER SHEATH WRINKLING

As described on page 16, four urania tubes failed during irradiation in the HWCTR by the formation of longitudinal wrinkles on the outer sheath. These failures occurred in tubes that had been compacted by vibration alone to rather low packed densities (82-87% TD) and then irradiated at moderate-to-high thermal ratings (37-49 watts/cm, peak). Volume reductions during irradiation indicated that, in each tube, the urania core densified to about 90% TD, thereby effectively shrinking the core within the sheath. The failure of the vibratory-compacted elements was attributed to plastic flow of the core during the densification process, which led to reduction in sheath support and consequent wrinkling of the outer sheath by the pressure of the coolant.

Cores swaged to 90% TD or greater will provide sufficient support to prevent collapse of the outer sheath of tubes operated up to at least 40 watts/cm. This conclusion is based on:

(a) Satisfactory performance of 7 swaged tubes operated at thermal ratings of 40-55 watts/cm (exposures to 4000 MWD/MTU).

(b) Negligible change in core density during irradiation of swaged tubes in (a) above, whereas cores of vibratory-compacted tubes that exhibited sheath collapse densified to about the density obtained by swage-compaction (90% TD).

(c) Negligible change in density of other swage-compacted and vibratory-compacted tubes irradiated to exposures of 14,000-17,000 MWD/MTU at thermal ratings between 17 and 25 watts/cm.

INNER SHEATH COLLAPSE

Early in the program, one urania tube failed by collapse of the inner sheath during irradiation in an SRP production reactor at low coolant pressure. After irradiation, the failed element contained an unusually large amount of fission and sorbed gas (67 cc of fission gas per kg and 108 cc of N_2 per kg), and the columnar grain structure of the core showed that the element had operated at an unusually high central temperature. The reason for the higher-than-expected operating temperature is not known; however, it is believed that a higher-than-normal release of sorbed gas from the core caused a pressure buildup that displaced the inner sheath and impaired the ability of the element to dissipate heat. The resulting increase in central temperature led to the release of additional gas which eventually caused the inner sheath to collapse.

The only other instance of inner sheath collapse resulted from a leaky weld as described on page 47 and occurred when the coolant pressure was removed after nuclear shutdown.

Urania fuel tubes fabricated by present techniques can probably operate in a power reactor at a rating of 30 watts/cm and reach burnups of 20,000 MWD/MTU without collapse of the inner sheath. This prediction is supported as follows:

(a) Sorbed gases in urania can be effectively controlled by outgassing during fabrication. The only impurity gas desorbed from the UO_2 in the current irradiations was nitrogen; in UO_2 that was vacuum outgassed at 1300°C or above, the release of nitrogen was less than 25 cc/kg UO_2. Hydrogen annealing was even more effective and should restrict release of impurity gases to less than 5 cc/kg UO_2; in three tubes containing hydrogen-annealed UO_2, the maximum release was 1 cc/kg UO_2. Thus the total amount of nonfission-product gas in irradiated tubes should not exceed 30-50 cc/kg UO_2.

(b) A urania tube compacted to about 90% of theoretical density and operated at 30 watts/cm will release about 25% of the fission gas formed during irradiation (Figure 6).

(c) Under the above conditions, the internal pressure during operation will be approximately 1300 psi at a burnup of 20,000 MWD/MTU, based on the following assumptions:

(1) No void chambers at the ends of the element.

(2) No axial flux gradient.

(3) A central temperature of 1600°C and a surface temperature of 400°C throughout the operating life of the element.

(d) The internal pressure in the fuel element must exceed the reactor operating pressure (assumed here to be 1500 psi) before a failure mechanism that depends upon displacement of the inner sheath to impair heat transfer can become effective.

For a full-length tube operating in a full-scale power reactor, the internal pressure will be less than calculated above because the axial flux gradient will reduce the average temperature in the element, and because void chambers can be used to provide additional free volume at the ends of the tube. However, for such tubes operating at moderate $\int k d\theta$'s, it is expected that the maximum allowable exposure will be limited by buildup of internal pressure even if each tube contains void chambers of reasonable size.

Results of calculations indicate that the inner sheaths of fuel tubes of interest will not collapse during reactor shutdown when the coolant pressure is removed. The internal pressures were calculated for various times after shutdown and compared with collapse pressures determined in out-of-pile tests. [6,18,19] For any reasonable mode of reactor shutdown, the calculated pressure in the element at the time of depressurization was always less than the collapse pressure.

HYDRIDE EMBRITTLEMENT OF ZIRCALOY SHEATHING

Sheath failures due to hydride embrittlement caused by an internal source of hydrogen were eliminated by incorporation of a drying step in the fabrication process for the urania tubes. Before the assembled tubes are swaged, they are dried at 250-275°C for approximately 20 hours. The residual moisture content of the core is less than 15 ppm. 110 tubes have been irradiated since the fabrication process was so modified with no repetitions of the earlier failures. Over 50 of these tubes were sectioned after irradiation; in all tubes, the Zircaloy sheaths were free of the type of hydriding that characterized the earlier failures.

APPENDIX A

SUMMARY OF IRRADIATION CONDITIONS FOR ALL UO_2 TUBES IRRADIATED IN THE HWCTR

Axial variation of peak ∫kdθ, time-weighted ∫kdθ, and exposure are shown in Figures A-1 through A-19 for each assembly of UO_2 tubes irradiated in the HWCTR. Points for the curves were computed from calorimetric data.

TABLE A-I

Characteristics and Irradiation Conditions of UO_2 Tubes in Assemblies That Were Not Examined after Irradiation

Tube No.	Oxide Core: Enrichment, % ^{235}U	Oxide Core: Vacuum Outgassing Treatment	Oxide Core: Method of Compaction	Oxide Core: Density, % TD	∫kdθ, watts/cm: Average in Time & Space	∫kdθ, watts/cm: Peak	Exposure, MWD/MTU: Average	Exposure, MWD/MTU: Max.
A. Base Case Tubes (approximately 2.1-in. OD, 1.5-in. ID)								
Short Tubes								
Assembly SOT-1-4								
ZE-228E	1.5	1 hr @ 1000-1100°C	V	84	7	19	3,900	5,000
ZE-229B	1.5	"	V	85	12	28	6,800	8,100
ZE-222H	1.5	"	V + S	91	18	30	10,000	11,200
ZE-222B	1.5	"	V + S	91	22	32	12,200	12,600
ZE-222D	1.5	"	V + S	90	22	32	12,300	12,700
ZE-232C	1.5	"	V	84	18	30	10,000	11,500
ZE-228C	1.5	"	V	85	10	21	5,700	7,800
Long Tubes								
Assembly OT-1-2								
ZE-223	1.5	1 hr @ 1000-1100°C	V + S	90	13	27	7,300	12,400
Assembly OT-1-3								
ZE-221	1.5	"	V + S	91	13	25	3,100	5,200
Assembly OT-1-4								
ZE-224	1.5	"	V + S	90	13	26	5,600	9,300
Assembly OT-1-5								
ZE-231	1.5	"	V	84	13	23	3,600	6,000
Assembly OT-1-6								
ZE-220	1.5	"	V + S	90	16	29	3,700	6,000
Assembly OT-1-7								
ZE-226	1.5	"	V + S	90	13	33	6,300	10,200
Assembly OT-3-2								
Z-215	Nat.	"	V	85	8	14	1,000	1,700
B. Reference Design Tubes								
Intermediate Size (2.5-in. OD, 1.8-in. ID)								
Assembly SOT-6-3								
Z-275B	Nat.	4 hr @ 1300-1400°C	V + S	92	9	20	,900	1,200
Z-276A	Nat.	"	V + S	91	16	27	1,700	2,000
Z-279C	Nat.	"	V + S	90	23	28	2,400	2,700
Z-278A	Nat.	"	V + S	92	27	30	2,700	2,700
Z-271B	Nat.	"	V + S	91	26	30	2,500	2,700
Z-276B	Nat.	"	V + S	91	18	26	1,900	2,200
Z-278B	Nat.	"	V + S	92	10	16	1,000	1,400
Large Size (3.7-in. OD, 3.0-in. ID)								
Assembly SOT-8-2								
ZE-288B	1.2	4 hr @ 1300-1400°C	V + S	91	7	19	1,200	1,700
ZE-293C	1.2	"	V + S	91	16	27	2,500	3,000
ZE-291A	1.2	"	V + S	91	24	26	3,500	3,800
ZE-289B	1.2	"	V + S	91	29	29	4,000	4,000
ZE-293B	1.2	"	V + S	91	25	29	3,700	3,900
ZE-293A	1.2	"	V + S	91	19	25	2,800	3,200
ZE-290C	1.2	"	V + S	91	10	14	1,400	2,000

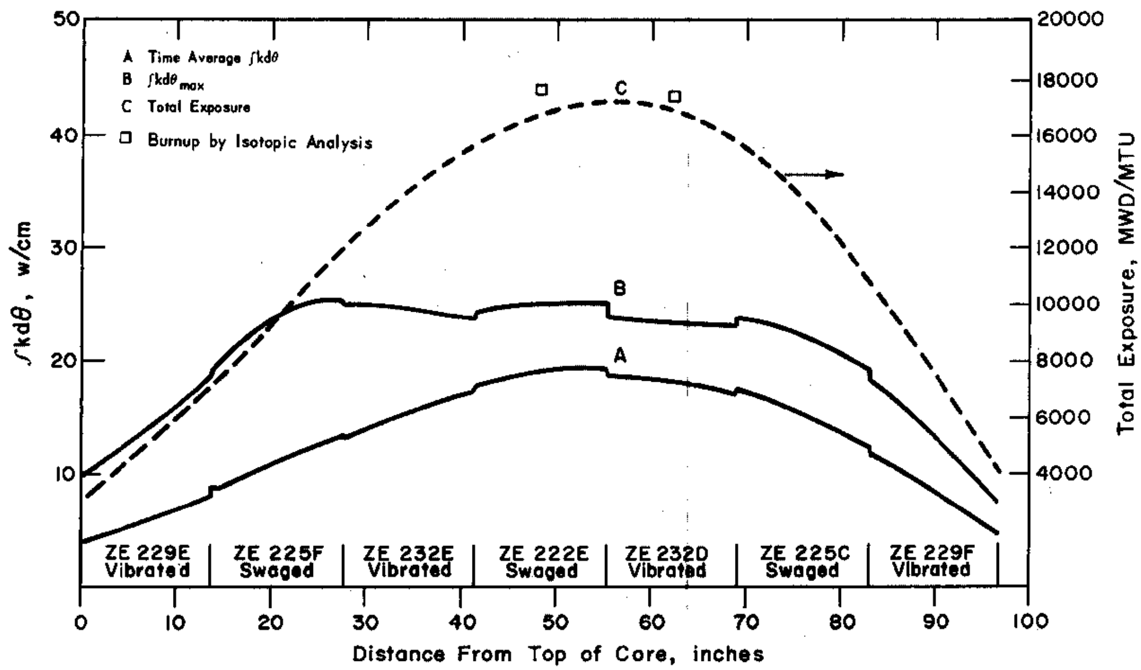

FIG. A-1 SOT-1-2

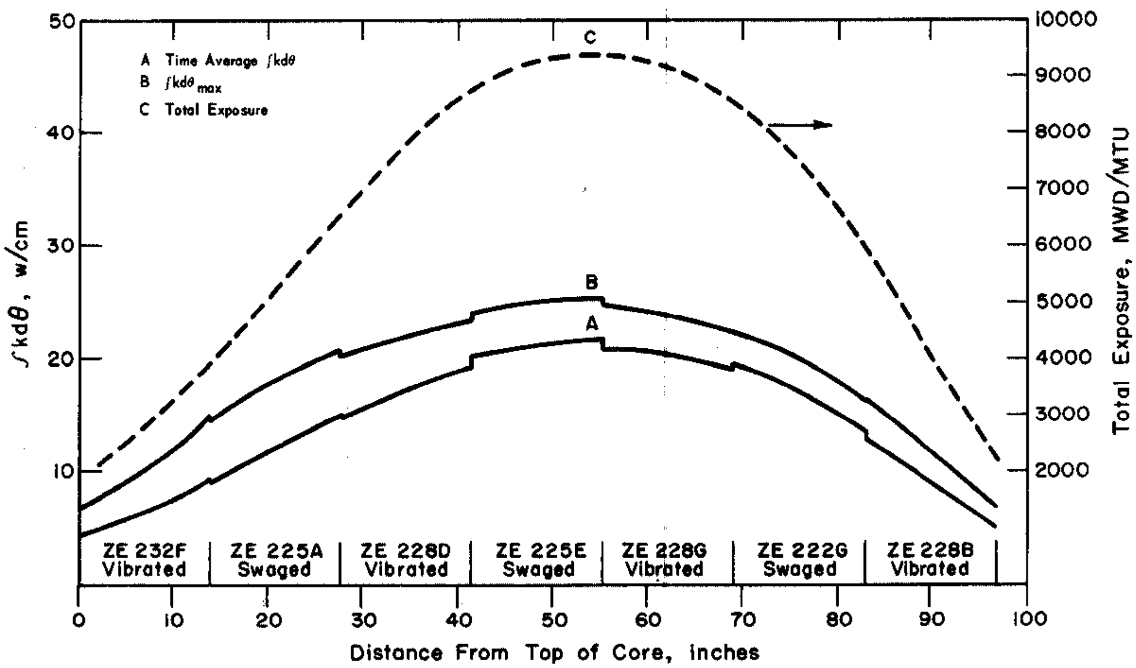

FIG. A-2 SOT-1-3

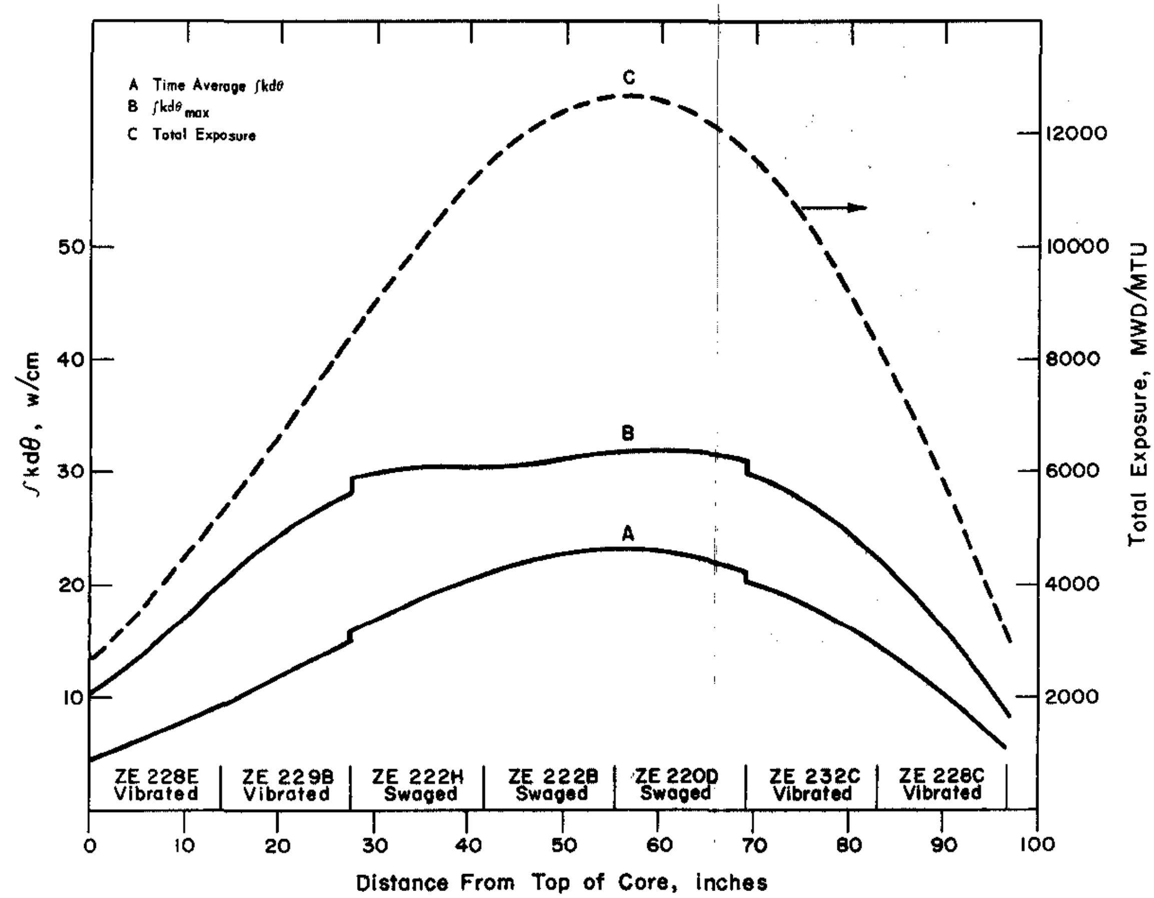
A Time Average ∫kdθ
B ∫kdθ max
C Total Exposure
C
B
A
∫kdθ, w/cm
Total Exposure, MWD/MTU
ZE 228E Vibrated
ZE 229B Vibrated
ZE 222H Swaged
ZE 222B Swaged
ZE 220D Swaged
ZE 232C Vibrated
ZE 228C Vibrated
Distance From Top of Core, inches

FIG. A-3 SOT-1-4

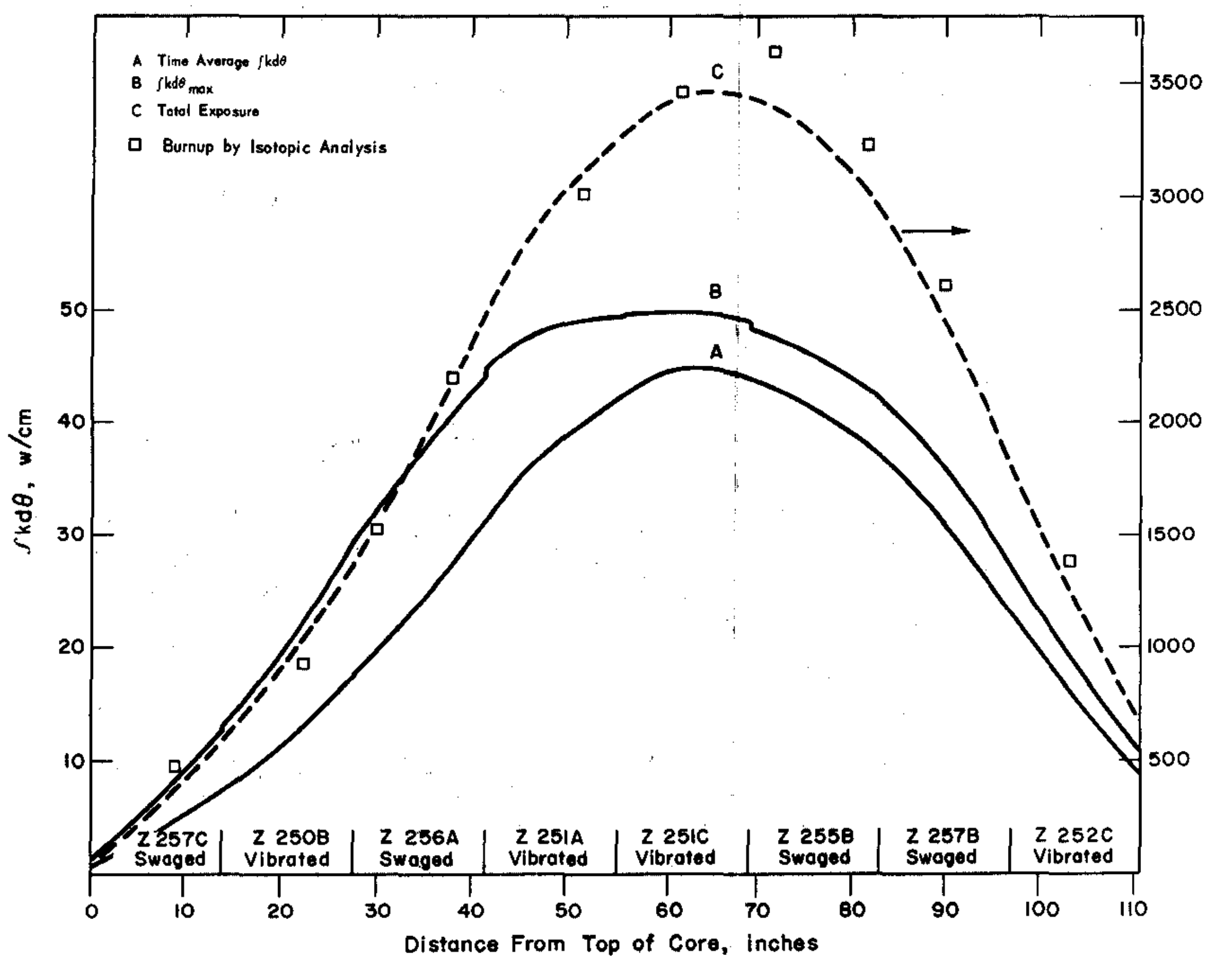

A Time Average ∫kdθ
B ∫kdθ max
C Total Exposure
□ Burnup by Isotopic Analysis
A
B
C
Z 257C Swaged
Z 250B Vibrated
Z 256A Swaged
Z 251A Vibrated
Z 251C Vibrated
Z 255B Swaged
Z 257B Swaged
Z 252C Vibrated
∫kdθ, w/cm
Total Exposure, MWD/MTU
Distance From Top of Core, inches

FIG. A-4 SOT-2-2

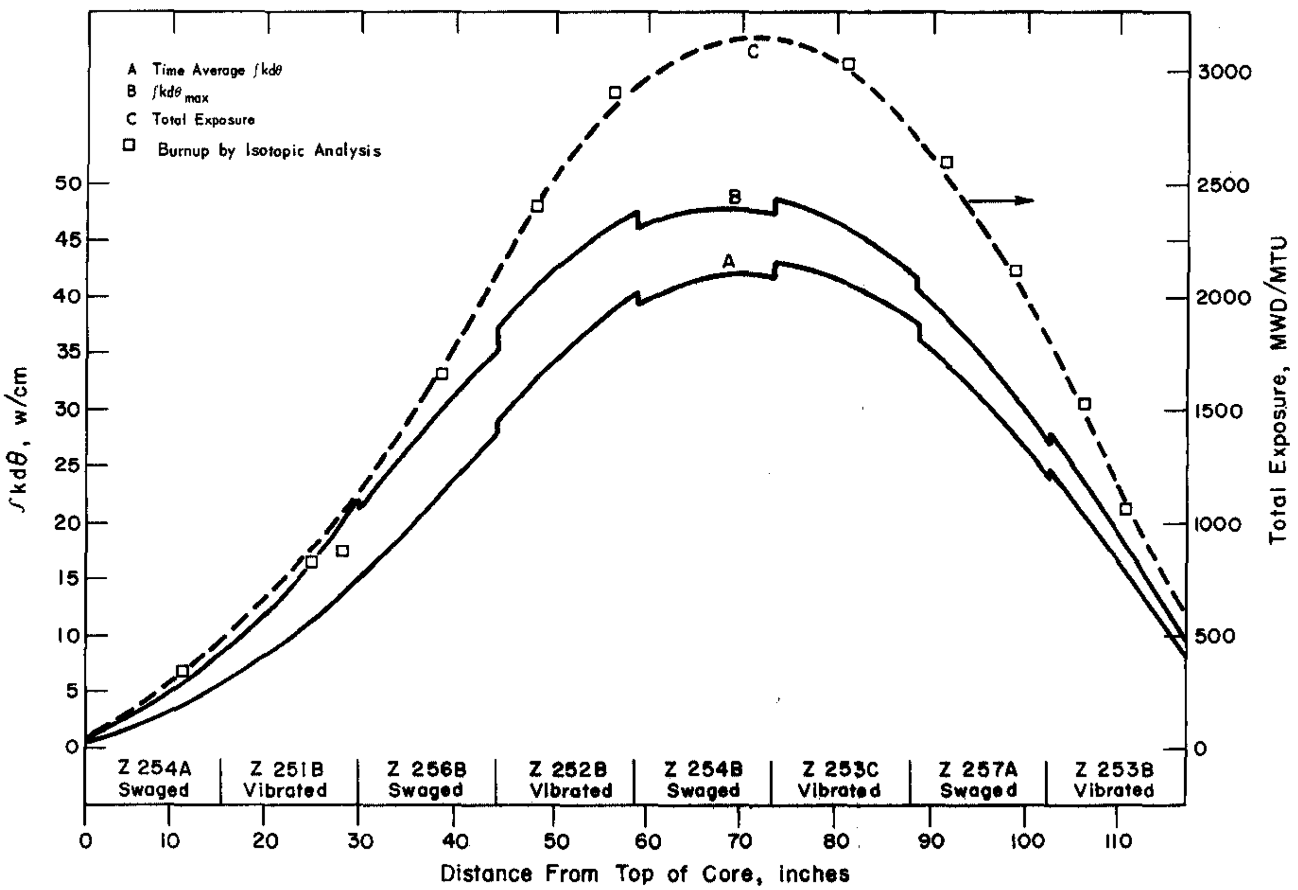
A Time Average ∫kdθ
B ∫kdθ max
C Total Exposure
Burnup by Isotopic Analysis
A
B
C
∫kdθ, w/cm
Total Exposure, MWD/MTU
Z 254A Swaged
Z 251B Vibrated
Z 256B Swaged
Z 252B Vibrated
Z 254B Swaged
Z 253C Vibrated
Z 257A Swaged
Z 253B Vibrated
Distance From Top of Core, inches

FIG. A-5 SOT-2-3

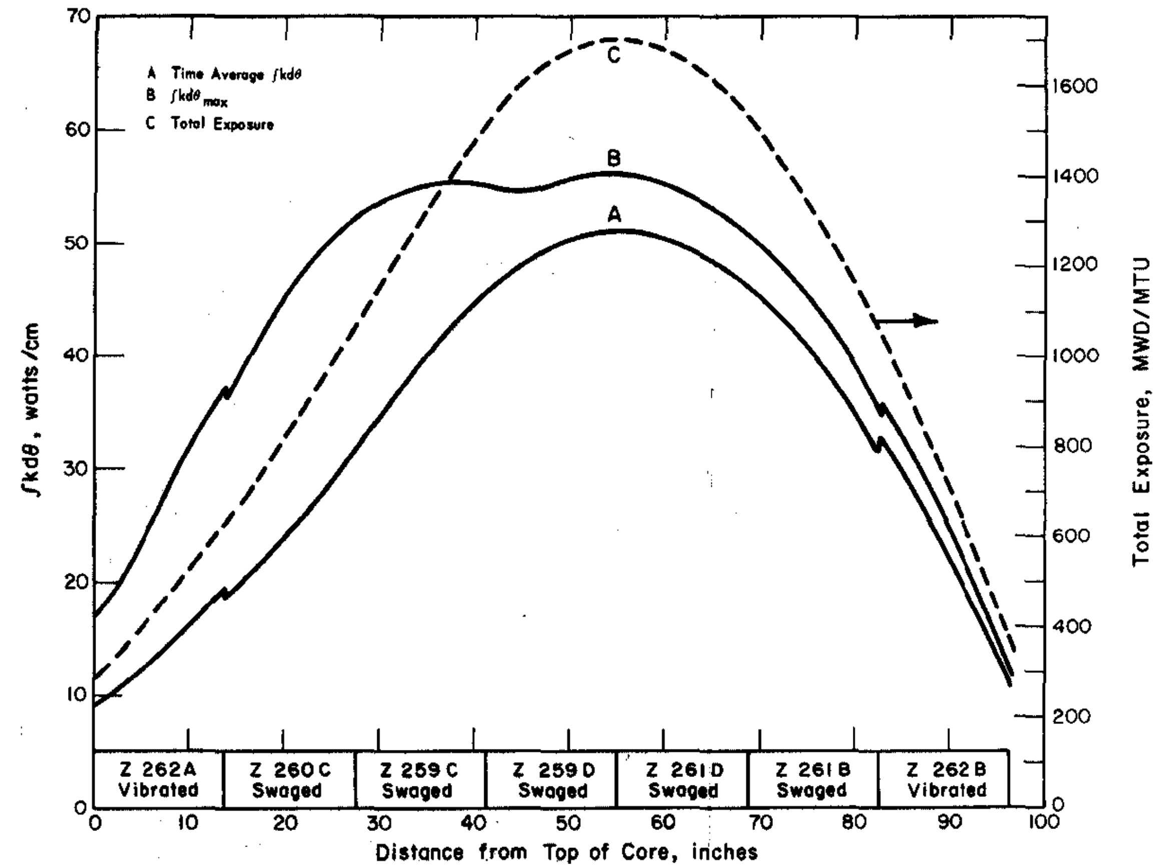

A Time Average ∫kdθ
B ∫kdθ max
C Total Exposure
C
B
A
∫kdθ, watts/cm
Total Exposure, MWD/MTU
Z 262A Vibrated
Z 260C Swaged
Z 259C Swaged
Z 259D Swaged
Z 261D Swaged
Z 261B Swaged
Z 262B Vibrated
Distance from Top of Core, inches

FIG. A-6 SOT-5-2

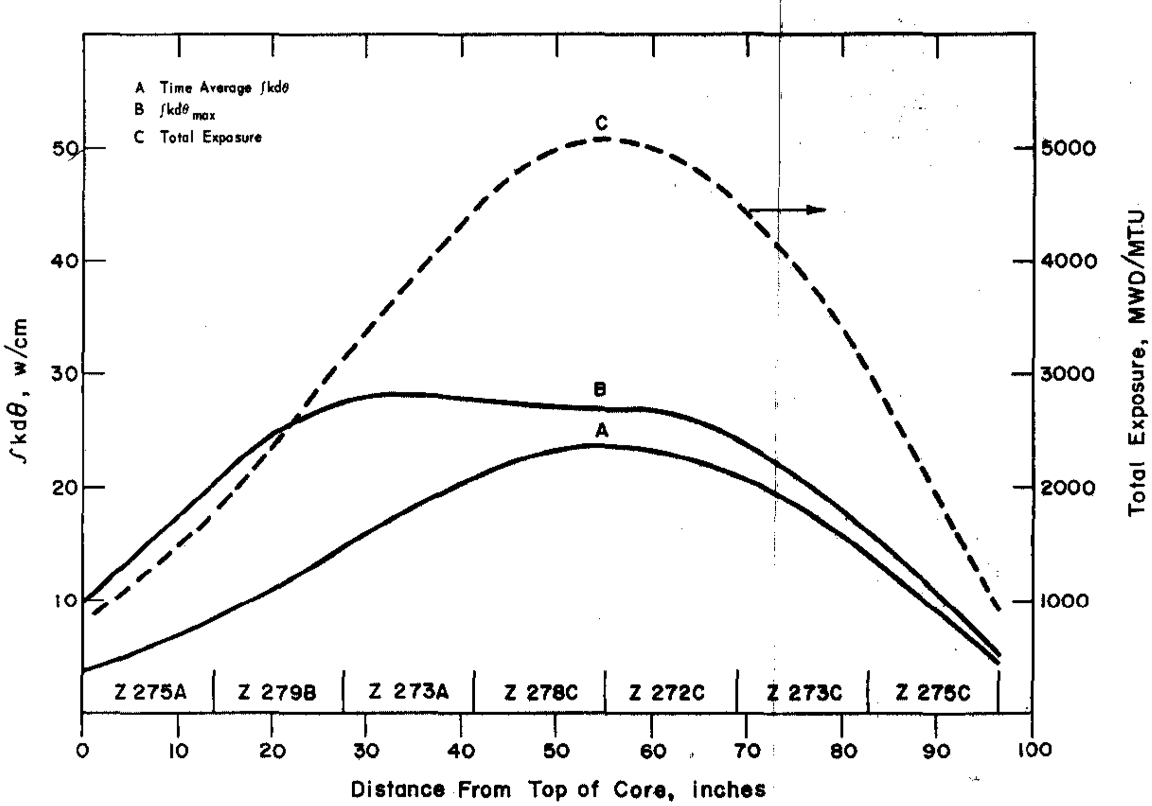

FIG. A-7 SOT-6-2 SWAGED

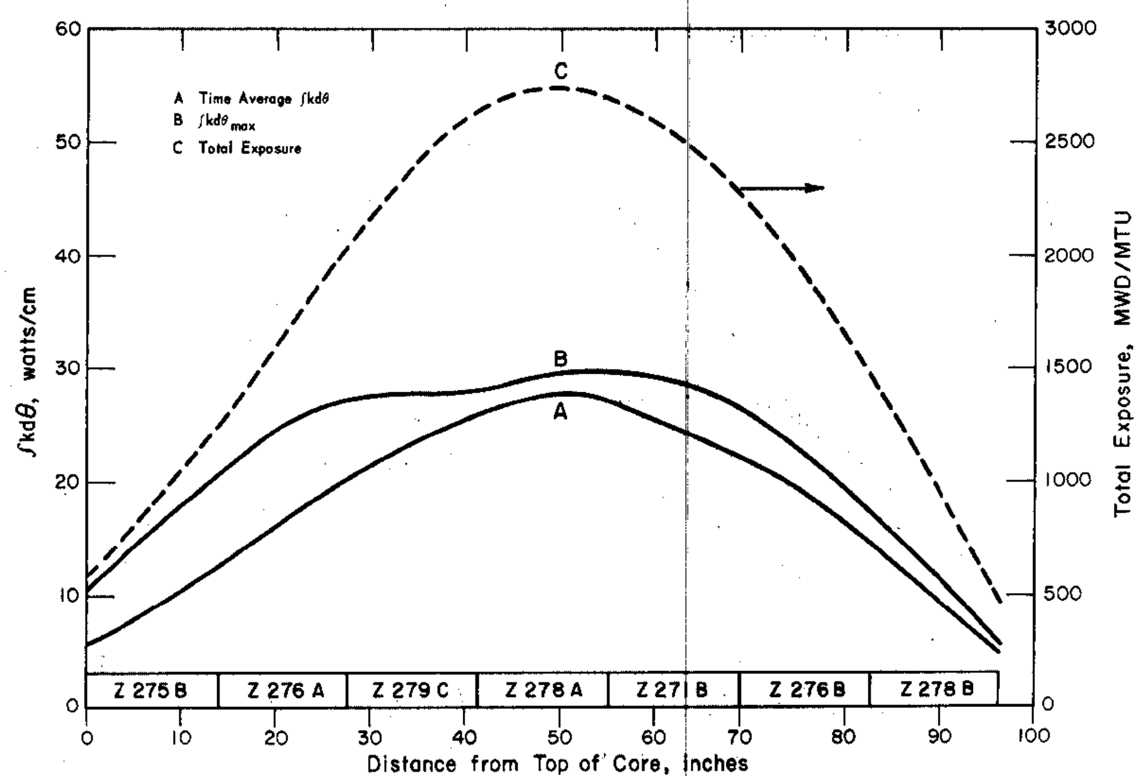

FIG. A-8 SOT-6-3 SWAGED

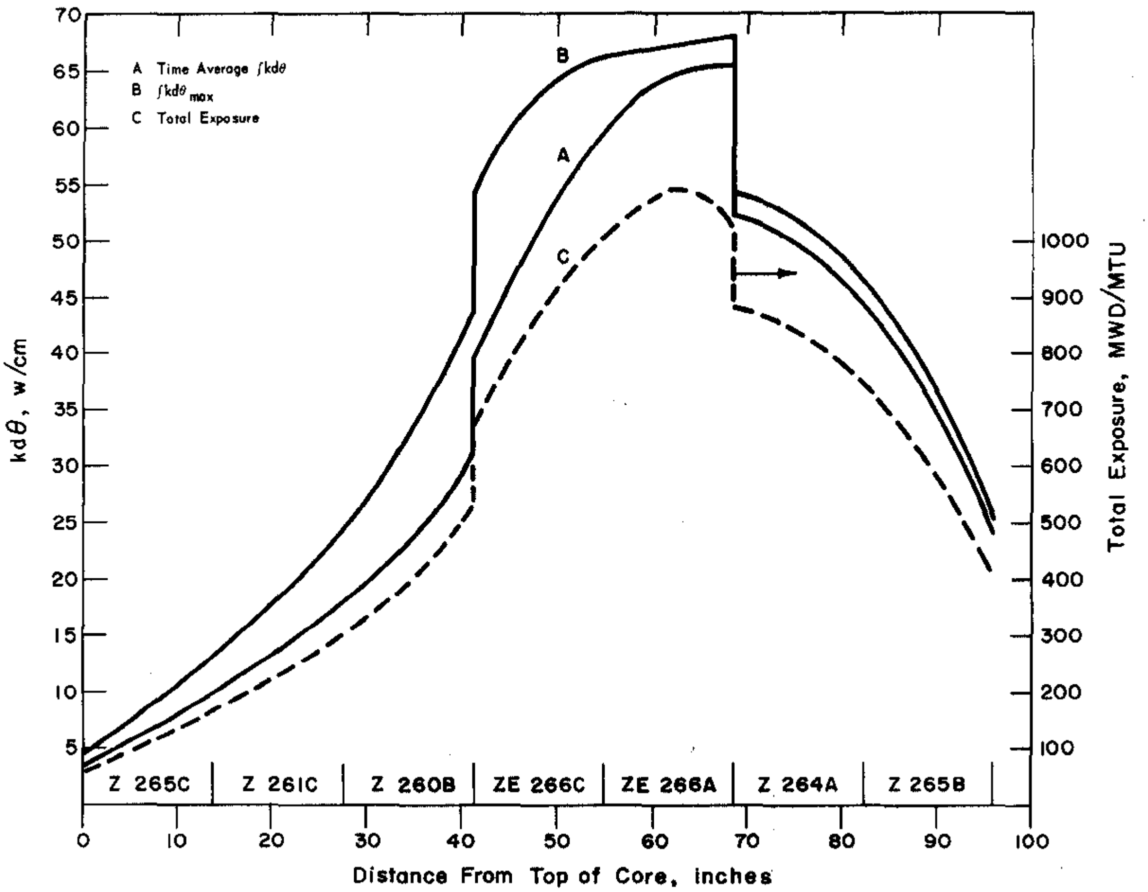

FIG. A-9 SOT-7-2 SWAGED

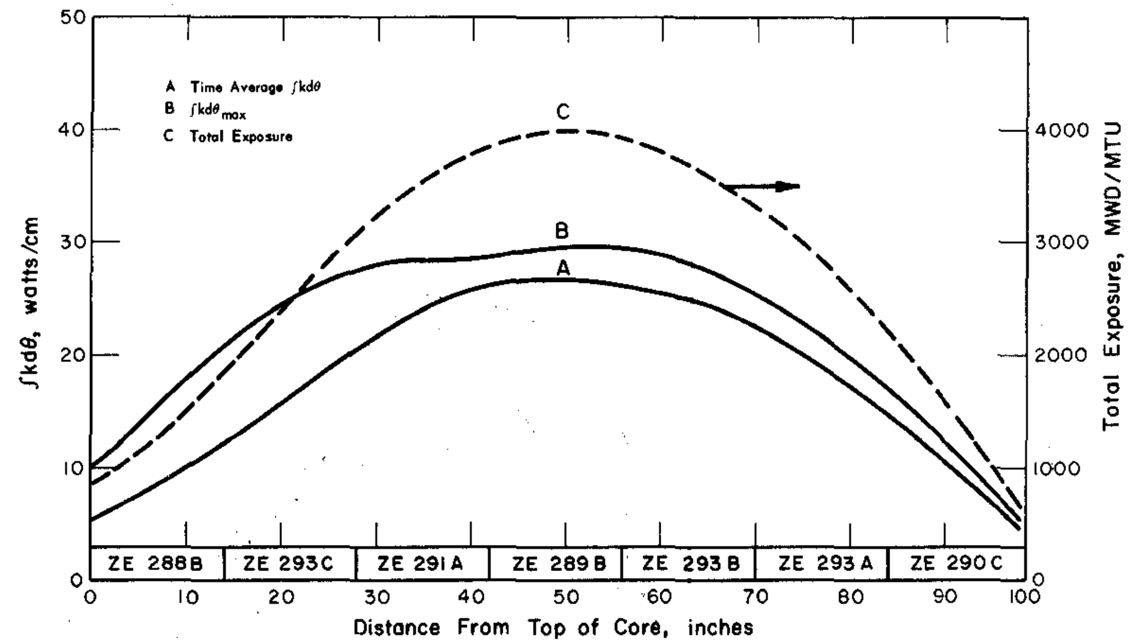

FIG. A-10 SOT-8-2

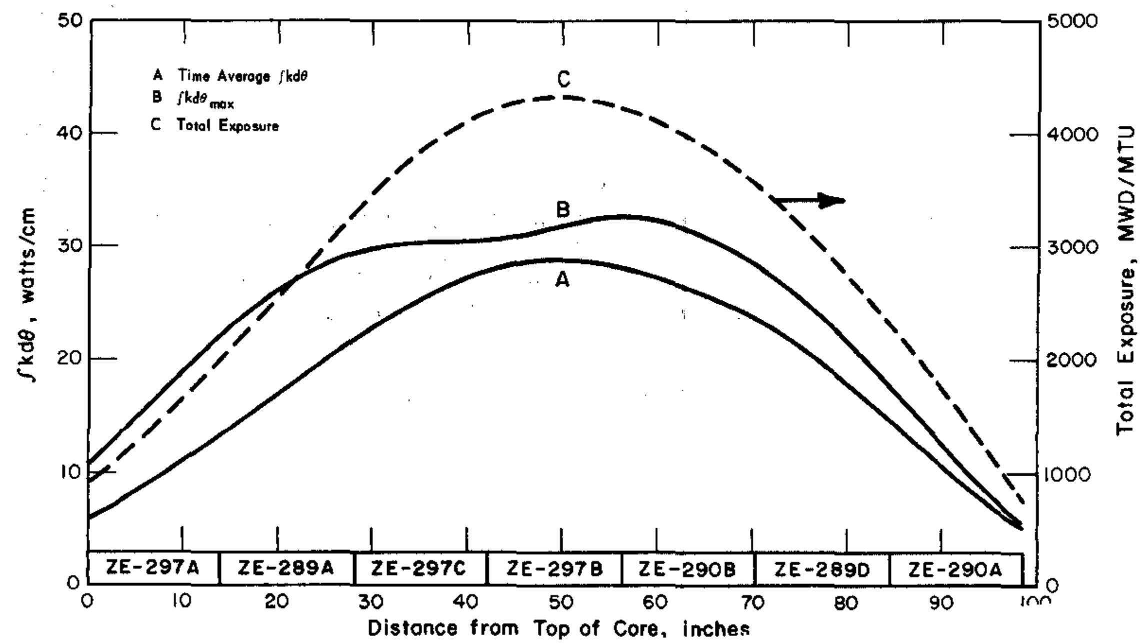

FIG. A-11 SOT-8-3

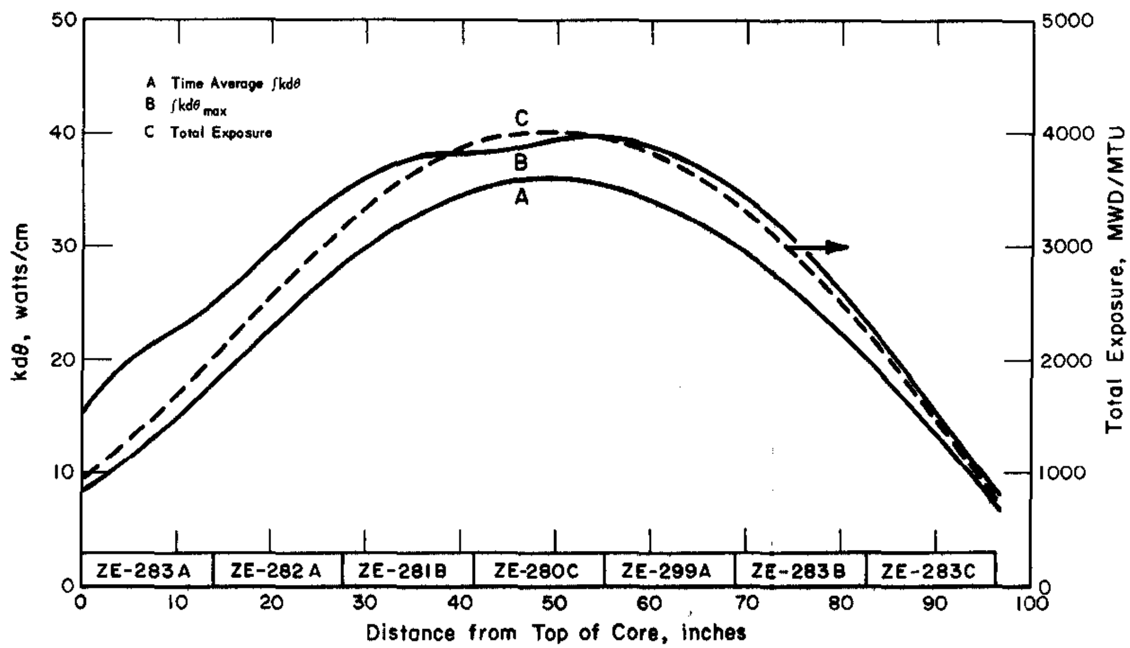

FIG. A-12 SOT-9-2 SWAGED

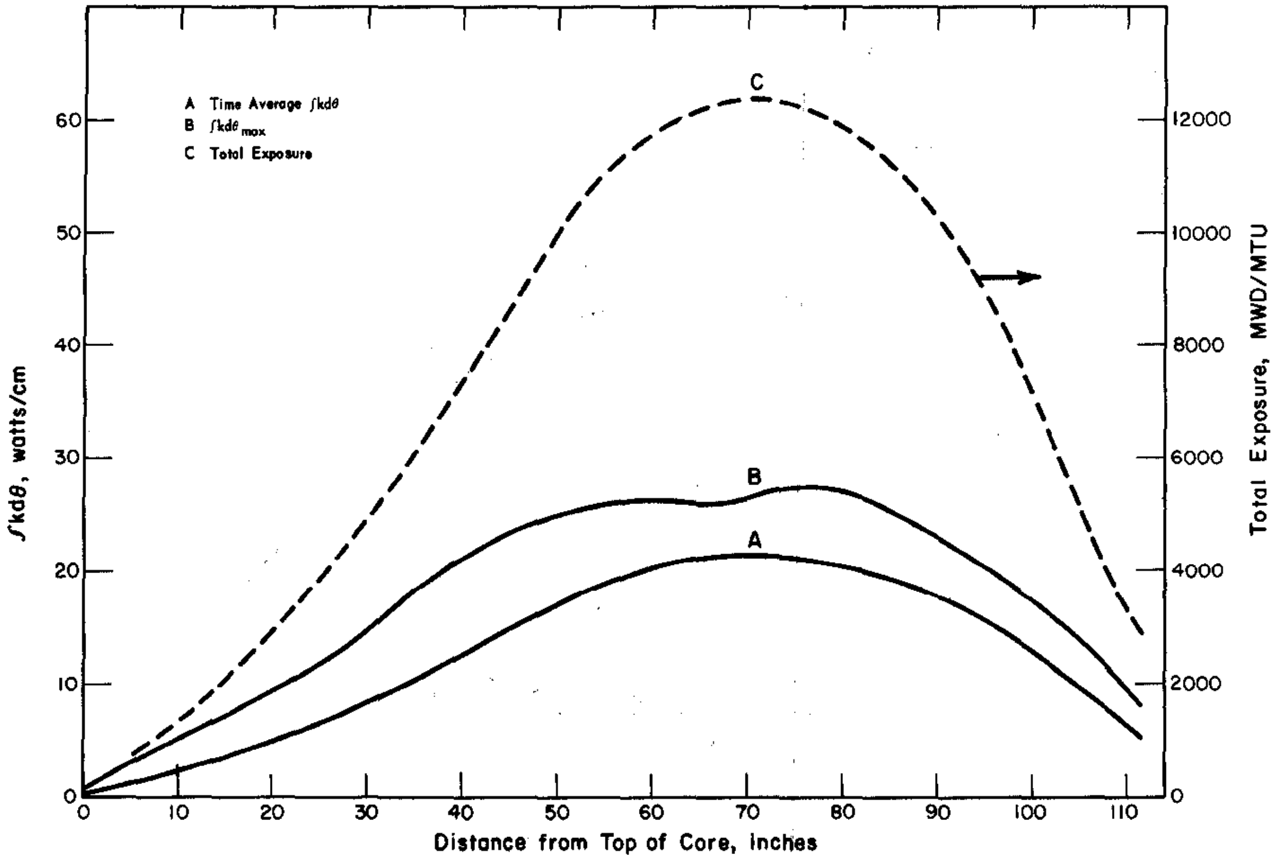

FIG. A-13 OT-1-2 SWAGED ZE-223

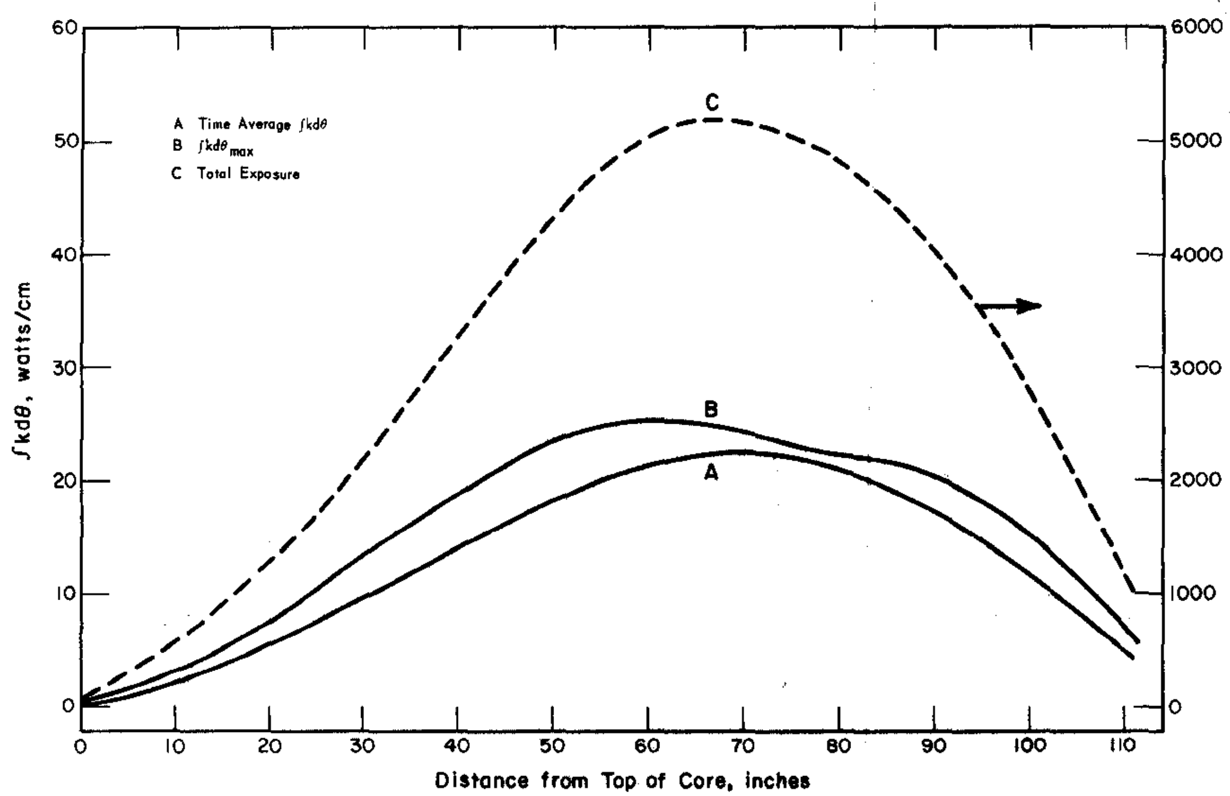

FIG. A-14 OT-1-3 SWAGED ZE-221

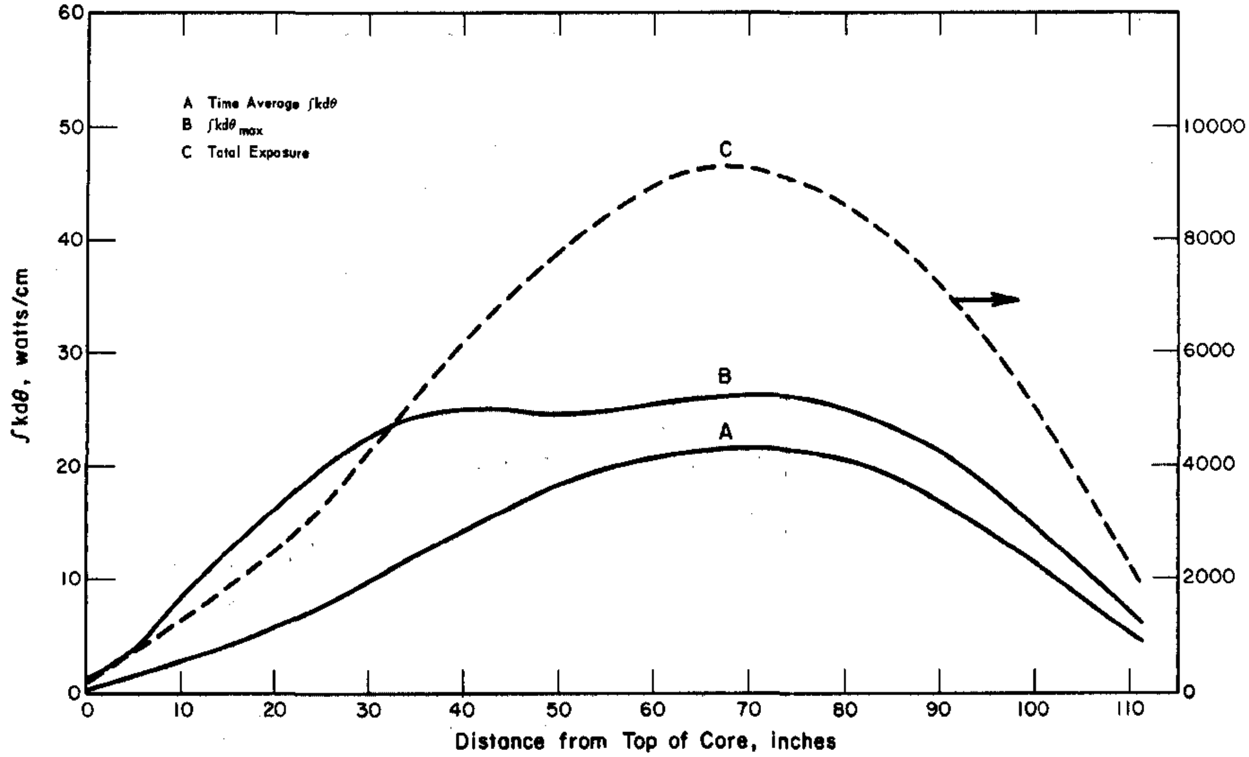

FIG. A-15 OT-1-4 SWAGED ZE-224

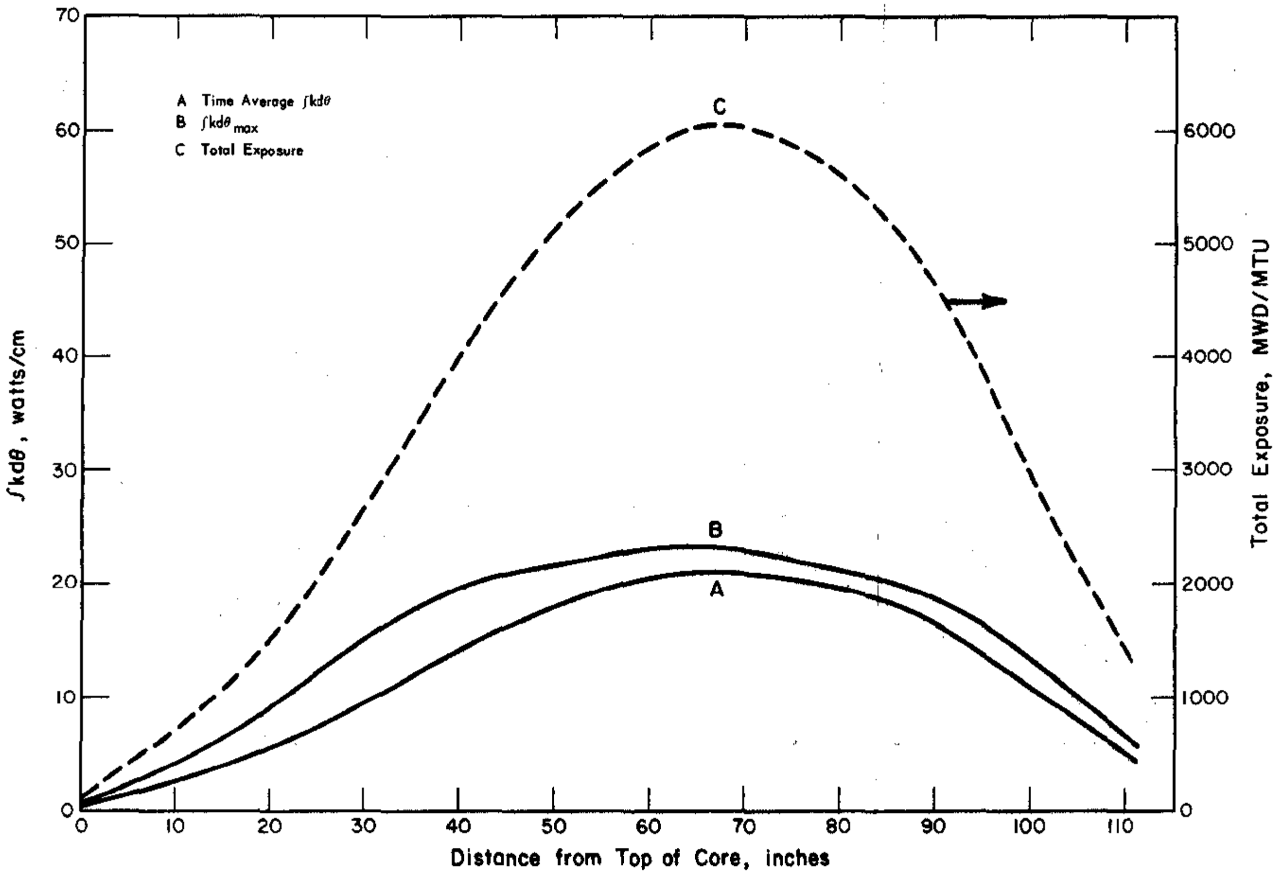

FIG. A-16 OT-1-5 VIBRATED ZE-231

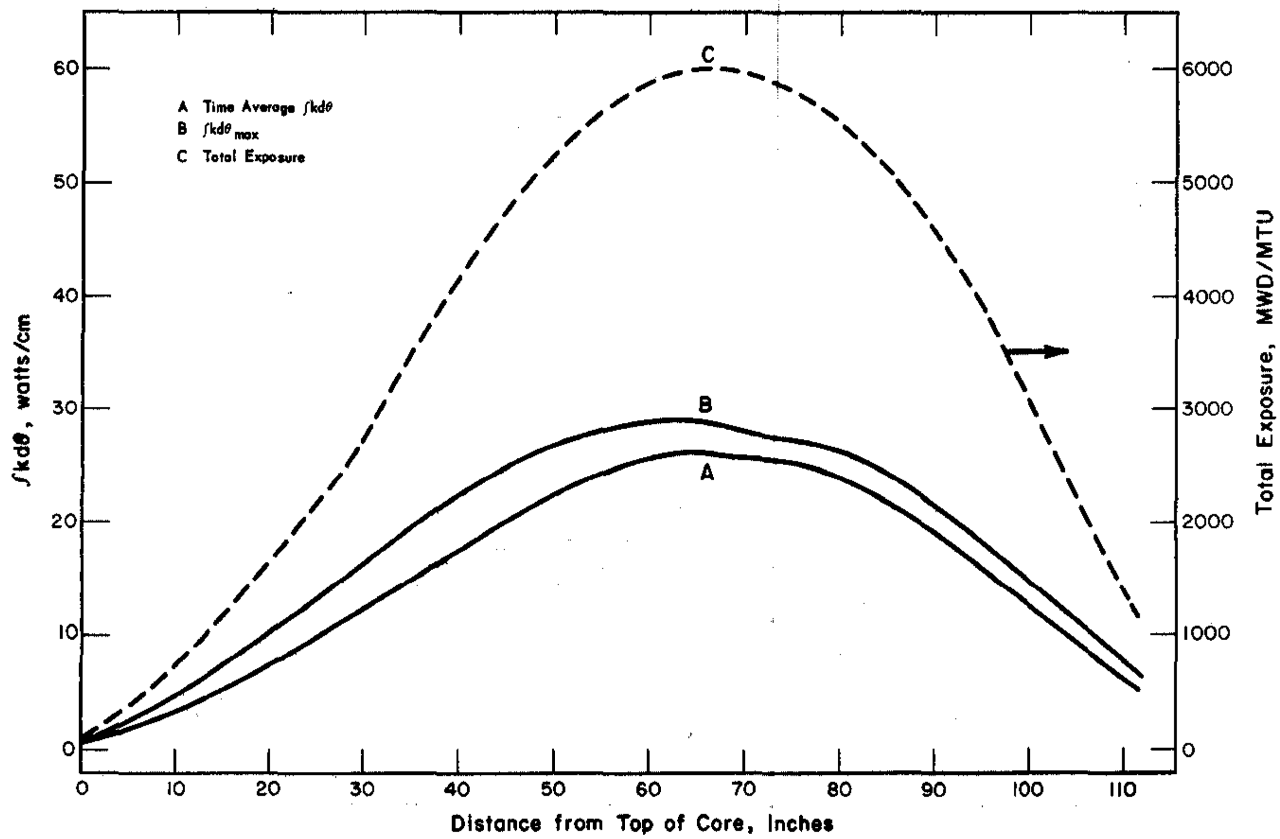

FIG. A-17 OT-1-6 SWAGED ZE-220

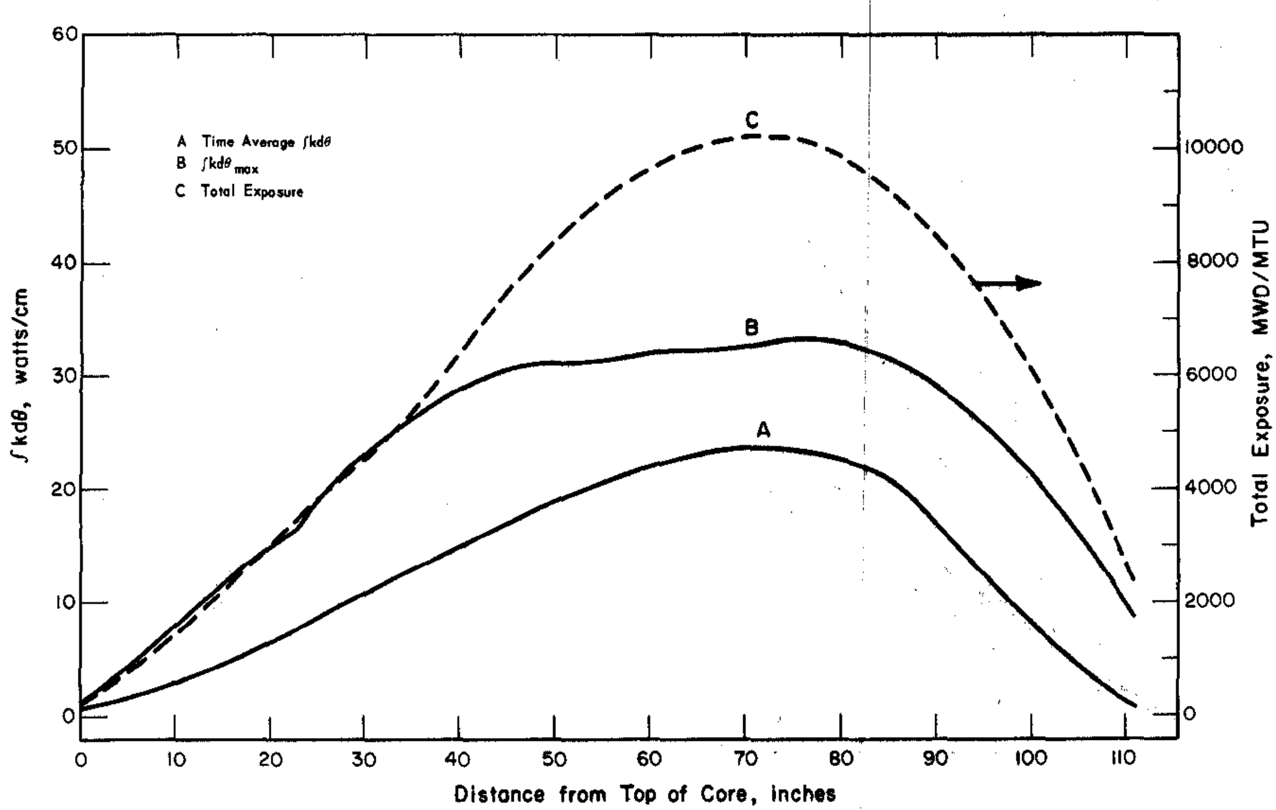

FIG. A-18 OT-1-7 SWAGED ZE-226

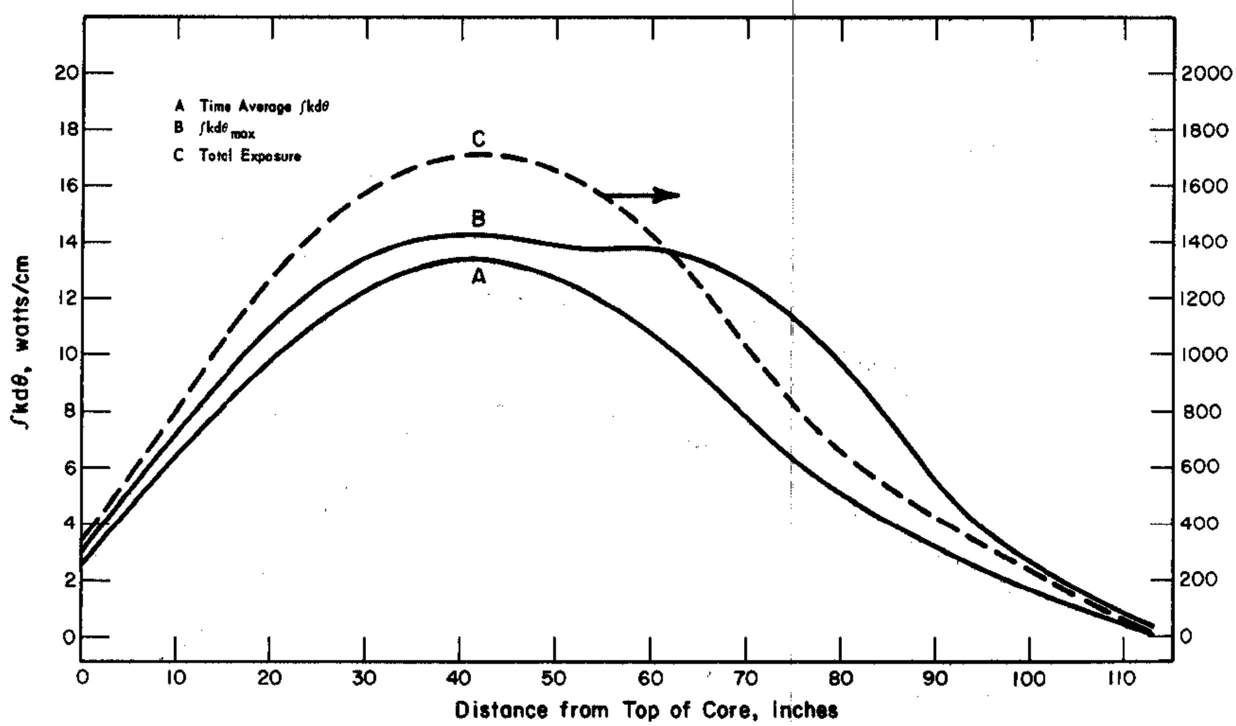

FIG. A-19 OT-3-2 VIBRATED Z-215

APPENDIX B

PROCEDURES FOR POSTIRRADIATION EXAMINATION

DIMENSIONS

After irradiation, the outside diameters, wall thicknesses and lengths of the tubes were measured with mechanical dial gage micrometers mounted on bases which also supported the tubes; the measuring devices were calibrated with standard blocks. Design and operation of the equipment for measuring outside diameters and wall thicknesses has been separately reported.[20,21] Equipment for measuring lengths consisted of 1) a horizontal V-block for supporting the tubes, 2) a vertical stop to establish a fixed reference point and to permit reproducible positioning of tubes and standard block, and 3) a dial gage micrometer mounted with the anvil bearing against the end of the tube at the "six o'clock" position. Thus, lengths could be measured at any angular position by rotating the tube about its axis.

VOLUME

Tube volumes were measured to provide additional information on irradiation-induced changes in size by determining the apparent gain in weight of a container of water when the tube was immersed in it. This method gave satisfactory precision and was more convenient for use in the hot cells than the standard method of determining the apparent loss in weight of an object immersed in a liquid of known density. Agreement of replicate volume measurements was generally within two cubic centimeters, or a few tenths of one percent.

GAS COLLECTION AND SAMPLING

The free gases contained in the irradiated tubes were determined by collecting the gas mixture in an evacuated system of known volume and analyzing the mixture in a mass spectrograph. The gas collection and sampling apparatus[22] consists of a chamber of a sufficient size to contain the fuel tube; a sharp steel punch (for piercing the outer sheath of the fuel tube) that is sealed to the sidewall of the chamber by stainless steel bellows and actuated by a hydraulic ram; a vacuum system comprising a pump and the usual pressure gages and valves; and a stainless steel sample bottle attached to the system by a ground tapered joint.

URANIUM BURNUP

Fuel exposures were calculated from reactor calorimetric data, and confirmed in a few cases by radiochemical or mass spectrographic analyses. Complete ring sections were analyzed to minimize errors due to migration of fission products; the sections were processed in 1/2- to 3/4-inch lengths to maintain integrity of the ring during cutting and handling prior to dissolution.

The methods for radiochemical and mass spectrographic analyses were based on those previously described.[23] For samples with a low calculated burnup, the determination was based on the concentration of fission product ^{137}Cs relative to the total uranium present. For samples with higher levels of burnup, the determination was based on the ^{235}U consumed relative to the amount initially present.

METALLOGRAPHY

Equipment and procedures used for metallographic examinations of sections from the urania cores and the Zircaloy sheaths of the irradiated fuel tubes have been described.[24] Details are given of the mounting, grinding, polishing, and etching procedures, with the exception of the chemical etch used for zirconium hydride platelets in Zircaloy. The etch consists of 30 ml conc HNO_3, 15 ml conc H_2O_2, 4 ml conc HF, and 50 ml H_2O, applied by swab for 5-10 seconds.

REFERENCES

1. D. F. Babcock, et al. An Evaluation of Heavy-Water-Moderated Power Reactors. USAEC Report DP-830, E. I. du Pont de Nemours and Co., Savannah River Laboratory, Aiken, S. C. (1963).

2. J. A. L. Robertson. ∫kdθ in Fuel Irradiations. Atomic Energy of Canada Limited Report CRFD-835, Chalk River, Ontario (1959).

3. G. R. Caskey, Jr., et al. "Failures of UO_2 Fuel Tubes by Internal Hydriding of Zircaloy-2 Sheaths," Symposium on Powder Packed Uranium Dioxide Fuel Elements. Joint US-Euratom Report CEND-153, Vol. II (1962).

4. R. R. Hood and L. Isakoff (compilers). Heavy Water Moderated Power Reactors, Progress Report, June 1962. USAEC Report DP-755, E. I. du Pont de Nemours and Co., Savannah River Laboratory, Aiken, S. C. (1962).

5. R. R. Hood (compiler). Heavy Water Moderated Power Reactors, Progress Report, September 1961. USAEC Report DP-665, E. I. du Pont de Nemours and Co., Savannah River Laboratory, Aiken, S. C. (1961).

6. R. R. Hood and L. Isakoff (compilers). Heavy Water Moderated Power Reactors, Progress Report, September 1962. USAEC Report DP-775, E. I. du Pont de Nemours and Co., Savannah River Laboratory, Aiken, S. C (1962).

7. H. C. Quigley. Irradiation of Uranium Dioxide Fuel Tubes in the VBWR. USAEC Report DP-837, E. I. du Pont de Nemours and Co., Savannah River Laboratory, Aiken, S. C. (1963).

8. A. S. Ferrara. Swaging of Uranium Dioxide Tubes - I. USAEC Report DP-493, E. I. du Pont de Nemours and Co., Savannah River Laboratory, Aiken, S. C. (1960).

9. H. G. Marsh. Fabrication of UO_2 Fuel Elements by Vibrational Compaction. USAEC Report DP-681, E. I. du Pont de Nemours and Co., Savannah River Laboratory, Aiken, S. C. (1962).

10. A. S. Ferrara. Uranium Dioxide Fuel Tubes for Irradiation in the VBWR. USAEC Report DP-989, E. I. du Pont de Nemours and Co., Savannah River Laboratory, Aiken, S. C. (1965).

11. A. S. Ferrara and W. G. Holmes. Development of Tubular UO_2 Elements for Power Reactors. USAEC Report DP-997, E. I. du Pont de Nemours and Co., Savannah River Laboratory, Aiken, S. C. (to be issued).

12. G. R. Cole. Influence of Thermal Rating and Bulk Density on Irradiation Performance of Fused UO_2 Tubular Fuel Elements. USAEC Report DP-1060, E. I. du Pont de Nemours and Co., Savannah River Laboratory, Aiken, S. C. (1966).

13. G. R. Cole. Evaluation of Fused UO_2. USAEC Report DP-819, E. I. du Pont de Nemours and Co., Savannah River Laboratory, Aiken, S. C. (1963).

14. G. R. Horn and J. A. Christensen. Identification of the Molten Zone in Irradiated UO_2. USAEC Report HW-SA-3055-Rev., General Electric Co., Hanford Atomic Products Operation, Richland, Wash. (1963).

15. R. R. Hood (compiler). Heavy Water Moderated Power Reactors, Progress Report, December 1961. USAEC Report DP-695, E. I. du Pont de Nemours and Co., Savannah River Laboratory, Aiken, S. C. (1962).

16. R. R. Hood and L. Isakoff (compilers). Heavy Water Moderated Power Reactors, Progress Report, January 1962. USAEC Report DP-705, E. I. du Pont de Nemours and Co., Savannah River Laboratory, Aiken, S. C. (1962).

17. J. W. Wade. A Computer Program for Economic Studies of Heavy Water Power Reactors. USAEC Report DP-707, E. I. du Pont de Nemours and Co., Savannah River Laboratory, Aiken, S. C. (1962).

18. R. R. Hood and L. Isakoff (compilers). Heavy Water Moderated Power Reactors, Progress Report, July 1962. USAEC Report DP-765, E. I. du Pont de Nemours and Co., Savannah River Laboratory, Aiken, S. C. (1962).

19. R. R. Hood and L. Isakoff (compilers). Heavy Water Moderated Power Reactors, Progress Report, May-June 1963. USAEC Report DP-855, E. I. du Pont de Nemours and Co., Savannah River Laboratory, Aiken, S. C. (1963).

20. C. E. Jackson. Gauge for Measuring Diameters of Irradiated Elements. USAEC Report DP-649, E. I. du Pont de Nemours and Co., Savannah River Laboratory, Aiken, S. C. (1961).

21. G. B. Cole. Gauge for Measuring Wall Thickness of Irradiated Tubular Elements. USAEC Report DP-761, E. I. du Pont de Nemours and Co., Savannah River Laboratory, Aiken, S. C. (1962).

22. P. H. Chismar. Fission Gas Sampler. USAEC Report DP-814, E. I. du Pont de Nemours and Co., Savannah River Laboratory, Aiken, S. C. (1963).

23. B. F. Rider, et al. The Determination of Uranium Burnup in MWD/Ton. USAEC Report GEAP-3373, General Electric Company, Vallecitos Atomic Laboratory, Pleasanton, California (1960).

24. R. D. Kelsch. "Hot Metallography Facility at Savannah River Laboratory," Proceedings of 11th Conference on Hot Laboratories and Equipment (American Nuclear Society), November 18-21, 1963.